



**Mercator
Ocean**
Ocean Forecasters

**SPECIAL ISSUE
with
Coriolis**



*The PRONUTS prototype is a tool allowing to autonomously profiling the nitrate concentrations in the ocean.
Credits: D'Ortenzio et al. this issue.*

Editorial – April 2012 – Special Issue jointly coordinated by *Mercator Ocean* and *Coriolis* focusing on Ocean Observations

Greetings all,

Once a year in April, Mercator Ocean in Toulouse and the Coriolis Infrastructure in Brest publish a common newsletter. Some papers are dedicated to observations only, when others display collaborations between the 2 aspects: Observations and Modelling/Data assimilation.

The two first papers are presenting two Equipex funded projects in order to better observe the ocean: The IAOS Ice Atmosphere Ocean Observing System over the Arctic Ocean (<http://www.iaos-equipex.upmc.fr>) and the NAOS (Novel Argo Ocean Observing system) (Le Traon et al.).

Then D'Ortenzio et al. are writing about the PRONUTS project aiming at autonomously profiling the nitrate concentrations in the ocean. During this project, two prototypes of PRONUTS will be developed and tested.

Next paper deals with a global glider infrastructure (EGO) for the benefit of marine research and operational oceanography (Testor et al.). Some key challenges have emerged from the expansion of the glider system and require now setting up a sustainable European as well as a Global system to operate glider and to ensure a smooth and sustained link to the Global Ocean Observing System (GOOS).

Vialard et al. are then displaying results about the Cirene oceanographic cruise, the part of the CLIVAR international effort to understand air-sea interactions at multiple time scales in the "Thermocline Ridge of the Indian Ocean" TRIO region.

Speich et al. follow with a paper about the use of ARGO floats to study the ocean dynamics south of Africa: what have been learnt from the Good-Hope project and what is planned within the SAMOC international programme.

Rio et al. then write about the use of altimetric and wind data to detect the anomalous loss of SVP-type drifter's drogue. They have developed a methodology that allows detecting the drifter drogue loss and providing an estimate of the wind slippage to be used as a velocity correction.

Surface salinity drifters for SMOS validation are also presented by Morisset et al. The surface drifters measuring sea surface salinity (SSS) in the top 50cm of the sea surface provide a complementary source of data for validating L-band sea surface salinity.

At last, a new information and data mining tool for North Atlantic Argo data is presented by Maze. This new tool aims at providing an interactive user interface for Argo data mining, simplifying access to information about all, or a sub-set of, profiles and centralizing as much as possible information provided by other services.

We will meet again next year in April 2013 for a new jointly coordinated Newsletter between Mercator Ocean and Coriolis. Note that there will not be exceptionally any publication of the newsletter in July this year. The next October 2012 issue will be about the NEMO ocean code recent developments.

We wish you a pleasant reading,

Laurence Crosnier and Sylvie Pouliquen, Editors.

CONTENT

NAOS: preparing the new decade for Argo.	3
<i>By P-Y. Le Traon, F. D'Ortenzio, M. Babin, H. Claustre, S. Pouliquen, S. Le Reste, V. Thierry, P. Brault, M. Guigue, M. Le Menn</i>	
Ice, Atmosphere, Ocean Observing System: the EQUIPEX-funded IAOOS project.	5
<i>By the IAOOS Team: C. Provost and J. Pelon, coordinators; P. Lattes scientific and technical project manager, J.C. Gascard, M. Calzas, F. Blouzon, A. Desautez, J. Descloitres, N. Sennéchaël, work package (co)-leaders, J.P. Pommereau, T. Foujols, A. Sarkissian, G. Ancellet, C. Drezen, A. Guillot, C. Guillermin, C. Berthold, N. Geyskens, A. Abchiche, N. Amarouche, L. Rey-Grange, J-M. Nicolas</i>	
Autonomously profiling the nitrate concentrations in the ocean: the pronuts project.	8
<i>By F. D'Ortenzio, S. Le Reste, H. Lavigne, F. Besson, H. Claustre, L. Coppola, A. Dufour, V. Dutreuil, A. Laës-Huon, E. Leymarie, D. Malardé, A. Mangin, C. Migon, P. Morin, A. Poteau, L. Prieur, P. Raimbault, P. Testor</i>	
EGO: Towards a global glider infrastructure for the benefit of marine research and operational oceanography.	12
<i>By P. Testor, L. Mortier, J. Karstensen, E. Mauri, K. Heywood, D. Hayes, P. Alenius, A. Alvarez, C. Barrera, L. Beguery, K. Bernardet, L. Bertino, A. Beszczynska-Möller, T. Carval, F. Counillon, E. Dumont, G. Griffiths, P. M. Haugan, J. Kaiser, D. Kasis, G. Krahmman, O. Llinas, L. Merckelbach, B. Mourre, K. Nittis, R. Onken, F. D'Ortenzio, S. Pouliquen, A. Proelss, R. Riethmüller, S. Ruiz, T. Sherwin, D. Smeed, L. Stemmann, K. Tikka, J. Tintoré</i>	
Cirene: from cyclones to interannual timescales in the south-western tropical Indian Ocean.	16
<i>By J. Vialard, Praveen Kumar B., N. C. Jourdain, and M. Bador</i>	
Use of ARGO floats to study the ocean dynamics south of Africa: what we have learned from the GoodHope project and what we plan within the SAMOC international programme.	21
<i>By Sabrina Speich, Michel Arhan, Emanuela Rusciano, Vincent Faure, Michel Ollitrault, Annaïg Prigent, Sebastiaan Swart</i>	
Use of altimetric and wind data to detect the anomalous loss of SVP-type drifter's drogoue	28
<i>By M-H. Rio</i>	
Surface salinity drifters for SMOS validation	33
<i>By S. Morisset, G. Reverdin, J. Boutin, N. Martin, X. Yin, F. Gaillard, P. Blouch, J. Rolland, J. Font, J. Salvador</i>	
A new information and data mining tool for North Atlantic Argo data	38
<i>By G. Maze</i>	

NAOS: PREPARING THE NEW DECADE FOR ARGO

By P-Y. Le Traon⁽¹⁾, F. D'Ortenzio⁽²⁾, M. Babin⁽³⁾, H. Claustre⁽²⁾, S. Pouliquen⁽¹⁾, S. Le Reste⁽¹⁾, V. Thierry⁽⁴⁾, P. Brault⁽⁵⁾, M. Guigue⁽⁶⁾, M. Le Menn⁽⁷⁾

¹ IFREMER, Brest, France

¹ UPMC/LOCEAN, Paris, France

³ CNRS/UMI Takuvik, Québec, Canada

⁴ UBO/IUEM/LPO, Brest, France

⁵ NKE, Hennebont, France

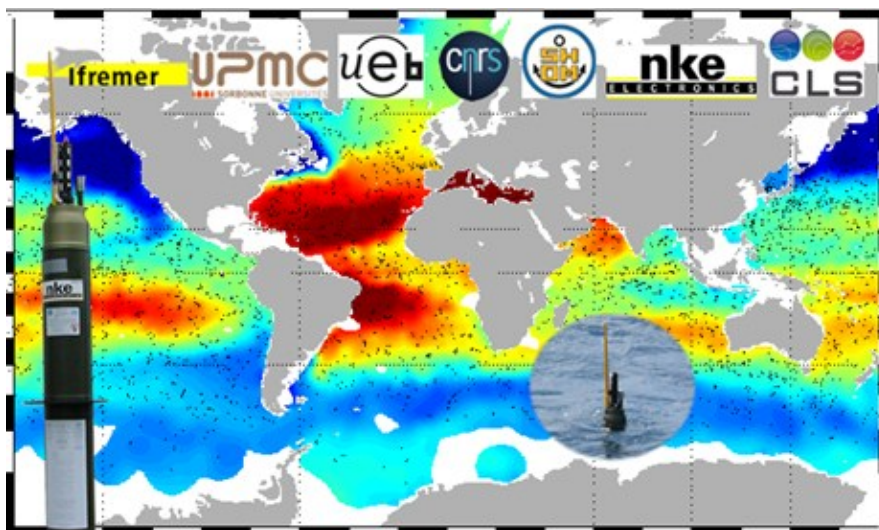
⁶ CLS, Toulouse, France

⁷ SHOM, Brest, France

NAOS (Novel Argo Ocean observing System) is one of the 52 projects selected as part of the *Equipex* call for proposals from the French *programme d'investissements d'avenir*. The overall objective of the project is to consolidate and improve the French and European contribution to the international Argo observing system and to prepare the next decade of Argo. The challenge is to set up an effective monitoring of the world ocean and to strengthen French leadership in ocean and climate research and prediction.

The project has two main objectives:

- To strengthen the French contribution to the Argo core mission (temperature and salinity from the surface down to 2000 m depth) by deploying between 10 to 15 additional floats per year over the 2012-2019 time period (110 floats in total). With the NAOS Argo floats, the French contribution to Argo will reach the target of 70 to 80 floats deployed each year.
- To develop, validate and deploy the next generation of French Argo profiling floats. 70 new generation floats will be deployed in three pilot areas: Mediterranean Sea, Arctic and North Atlantic. New float capabilities will include: more efficient design of the vehicle, improved transmission rates, integration of biogeochemical sensors, deeper measurements and under ice operations in the polar seas.



NAOS is a partnership between Ifremer (coordinator), UPMC (co-coordinator), CNRS, UBO/IUEM (PRES UEB), SHOM, CLS and the SME NKE. The scientific coordination of the project is ensured through a scientific steering committee co-chaired by P.Y. Le Traon and F. D'Ortenzio. This committee met twice (September 23rd, 2011 and January 4th, 2012). The steering committee refers to a governing board. The first governing board meeting was held on January 4th, 2012.

The project is organized around five main work packages:

- WP1: Consolidation of the French contribution to Argo (resp. S. Pouliquen)
- WP2: Development of the new generation of French Argo floats (resp. S. Le Reste)
- WP3: Floats with biogeochemical sensors in the Mediterranean Sea (resp. F. D'Ortenzio)
- WP4: Floats with biogeochemical sensors in the Arctic (resp. M. Babin)
- WP5: Deep floats with oxygen sensors in the North Atlantic (resp. V. Thierry).

The project started in June 1st, 2011 and will end in December 2019. Development and testing of prototypes will be conducted in WP2 from June 2011 to June 2014. Procurement of floats for WP1, 3, 4 and 5 will be done from January 2012 to January 2016. The first WP1 and WP3 series (2012 and 2013) will use existing models of French Argo floats (Provior and Arvor). The following series will benefit from WP2 advances. WP4 and WP5 floats will be solely based on new models developed in WP2.

NAOS is now well on track. The project office was set up, the WWW site developed (<http://www.naos-equipex.fr>) and the first communication actions have started. Project tasks have entered an intensive phase: float technical specifications, testing, procurement for the first

prototypes, tenders or orders of the first series, actions to improve at sea monitoring tools, protocols for validation and testing of floats, etc

The involvement of the wider French oceanography community through the *Groupe Mission Mercator Ocean Coriolis* (GMMC) will be essential to the success of NAOS. Interactions are first needed so that the new NAOS floats meet expectations from the GMMC. Array design studies (e.g. OSSEs) for the next generation of Argo floats (biogeochemical, deep and Arctic floats) should also be conducted as part of GMMC activities. On the longer run, a strong involvement of GMMC groups in the data analysis of the new floats (prototypes and series) will be essential. Developing the use and testing the impact of NAOS floats in Mercator Ocean data assimilation systems will also be critical.

To ensure a good interaction between NAOS and the GMMC, NAOS is regularly discussed during the Mercator Ocean/Coriolis scientific council meetings and Coriolis executive committee meetings. NAOS activities will be presented regularly at GMMC meetings and NAOS annual meetings will be open to the GMMC. The NAOS meeting in 2012 will be held at Ifremer in Brest on June 21st and 22nd. All GMMC groups are strongly invited to participate !

For more information on the NAOS project, see <http://www.naos-equipex.fr> or contact us at naos@ifremer.fr

Acknowledgments

NAOS benefits from the *programme d'investissements d'avenir* funding from the French government. This contribution is organized by the *Agence nationale de la recherche* (ANR-10-EQPX-40).



ICE, ATMOSPHERE, OCEAN OBSERVING SYSTEM: THE EQUIPEX-FUNDED IAOOS PROJECT

By the IAOOS Team: C. Provost⁽¹⁾ and J. Pelon⁽²⁾, coordinators; P. Lattes⁽¹⁾ scientific and technical project manager, J.C. Gascard⁽¹⁾, M. Calzas⁽³⁾, F. Blouzon⁽³⁾, A. Desautez⁽⁴⁾, J. Descloitres⁽⁵⁾, N. Sennéchaël⁽¹⁾, work package (co)-leaders, J.P. Pommereau⁽²⁾, T. Foujols⁽²⁾, A. Sarkissian⁽²⁾, G. Ancellet⁽²⁾, C. Drezen⁽³⁾, A. Guillot⁽³⁾, C. Guillerm⁽³⁾, C. Berthold⁽³⁾, N. Geyskens⁽³⁾, A. Abchiche⁽³⁾, N. Amarouche⁽³⁾, L. Rey-Grange⁽³⁾, J-M. Nicolas⁽⁵⁾

¹ UPMC/LOCEAN, Paris, France

² LATMOS, Paris and Guyancourt, France

³ INSU, Brest and Meudon, France

⁴ IPEV, Brest, France

⁵ ICARE, Lille, France

Context

The most conspicuous manifestations of the current climate warming are found in the Arctic. The warming trend in the Arctic is almost twice as large as the global average in recent decades. This is known as Arctic amplification. Changes in cloud cover, increases in atmospheric water vapor, more atmospheric heat transport from lower latitudes and declining sea ice have all been suggested as contributing factors. The extreme reduction of the Arctic sea-ice cover at the end of the summer has a huge impact on the Earth radiation budget and fluxes at the air-surface interface. It is responsible for a warming of the upper ocean and of the lower atmosphere, a change of the atmospheric circulation (polar vortex and storm tracks), an increase of cold air outbreaks enhancing heat flux release and low cloud formation and sudden stratospheric warming events, an acceleration of Greenland ice melting and sea level rise and an increase of permafrost thawing releasing large amount of greenhouse gases into the atmosphere. Shifts in wind regime, accelerating sea-ice motion, increasing sea-ice deformation, fracturing and ridging, producing more open waters, diminishing the albedo and increasing absorption of solar radiation by the upper ocean also contribute to amplified sea-ice changes in the Arctic. To interpret the Arctic amplification, pan-Arctic measurements in the water column, sea-ice and overlying atmosphere are needed.

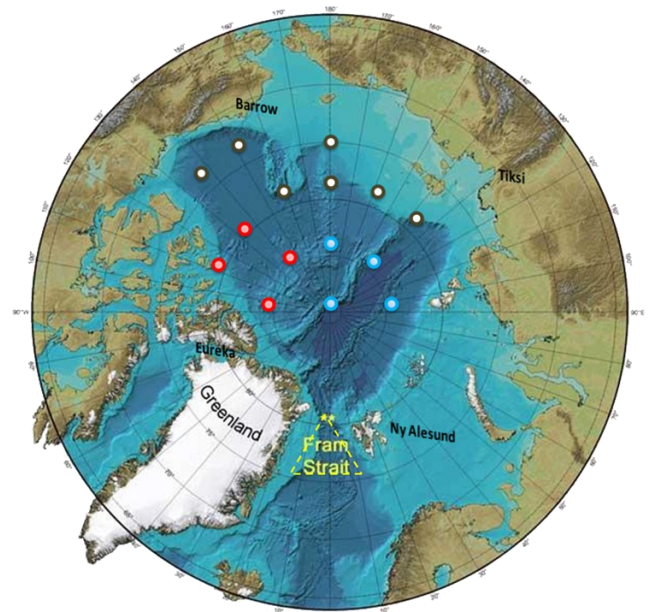
Objectives

The main objective of the IAOOS project is to provide and to maintain an integrated observing system over the Arctic Ocean to collect synoptic and near real time information related to the state of the upper ocean, the lower atmosphere and the Arctic sea-ice. These data are complementary to satellite observations and models.

In the ocean we are targeting the first 1000m beneath the surface to document precisely the surface mixed layer, the halocline and the Atlantic and/or Pacific water masses advected into the Arctic Ocean via Fram Strait and Bering Strait respectively. In the sea-ice we need to document few meters to infer temperature profiles through the ice layer and the sea-ice thickness as a function of time in order to control sea ice melting and freezing and sea-ice deformation. In the atmosphere we do not have actually any system able to profile throughout the troposphere and up to the stratosphere except from satellites. However, profiles obtained in the lower troposphere from satellites are subject to errors and bias. So we need automatic profilers operated from the ground and looking upward.

The IAOOS system involves 15 autonomous platforms operating at any given time in the Arctic Ocean for a period of 7 years in total. Each platform is composed of 3 elements for oceanographic, sea-ice and atmospheric vertical soundings (Figure 2). The platforms are designed to float at the surface of the ocean as well as to remain on top of sea-ice floes. The target for their autonomy is two years.

The fifteen IAOOS platforms will be drifting according to sea-ice motion, surface winds and ocean currents and it will be necessary to replace part of the fifteen platforms every year. It is anticipated that six platforms will either drift away from the central Arctic Ocean through Fram Strait or be destroyed by sea-ice rafting or ridging every year. It is planned to replace six platforms every year during five years following an initial deployment of fifteen platforms. This will amount to a total of forty IAOOS platforms for the entire duration of the experiment.



- Fall deployment by Ship logistics
- Spring deployment by Air logistics (NY ALESUND)
- Spring deployment by Air logistics (EUREKA)

Figure 1: Ideal distribution of the 15 IAOOS platforms

Partnership:

IAOOS results from a cooperation between Université Pierre and Marie Curie (UPMC, www.upmc.fr), coordinator with two laboratories involved LOCEAN (www.locean-ipsl.upmc.fr) and LATMOS (www.latmos.ipsl.fr), the Technical Division from CNRS-INSU (DT-INSU, www.dt-insu.cnrs.fr), the Institut Paul Emile Victor (IPEV, www.institut-polaire.fr) and the atmosphere data center in Lille ICARE (www.icare.univ-lille1.fr). Instrument developers and providers include several companies: NKE (www.nke-corporate.fr), CIMEL (www.cimel.fr), SAMS (www.SAMS.ac.uk), MOBILIS (<http://www.mobilis-sa.com/>)...

Close ties are developed with Coriolis data centre (<http://www.coriolis.eu.org/>) and equipex NAOS work package 4 (<http://www.naos-equipex.fr/>).

The project started in October 2011 and will end in December 2019.

Structure of the project

IAOOS is organized in 5 work packages (Figure 3).

WP1 : Ocean measurements

The system is composed of a surface buoy unit capable of floating at the surface of an ocean free of ice as well as being deployed on sea-ice. This surface unit contains the GPS and Iridium transmitters for geo-localization and real time data transmission to dedicated satellites. It also contains the processor for data acquisition and the lithium battery supply for a two-year operation. A 800-m long cable is attached to the buoy underneath and loaded with a 50 kg deadweight at the very end in order to keep the cable as vertical as possible even during strong sea-ice drift entraining the surface buoy and the 800-m long cable. Along this 800-m long cable an ARGO-like float equipped with a CTD is scanning up and down from surface down to 800 m depth and up, taking vertical profiles of temperature and salinity once or twice per day. At the end of each profile, the data are immediately transmitted by Iridium to satellites and to land. These profiles are very important to keep us informed about the ocean mixed layer depth, the depth and strength of the halocline, the Atlantic layer and/or the Pacific layer under the halocline. These are fundamental observations in order to compute the heat flux from the ocean to the ice or to the atmosphere. A synergy is being developed with work package 4 of NAOS (www.naos-equipex.fr) to deploy floats with biogeochemical sensors onto IAOOS platforms.

WP2 : Ice measurements

IAOOS platforms measure sea-ice thickness, snow depth and temperature profiles across the air-sea-ice interfaces. Unfortunately no satellite sensor can directly measure ice thickness. It is essential that long-term, high-quality observational measurements, which encompass the annual cycle of growth and decay of sea ice (Ice mass balance or IMB), be performed. Only then will we be able to understand the processes involved and to validate and refine the models. This can only be performed through the development of a basin-wide network of reliable and affordable autonomous instrumentation. Thus the equipment for sea-ice is based on a combination of satellites (AMSR-E, Cryosat etc..) and a thermistor-heater chain from SAMS. The 6-meter-long chain comprises thermistors and heaters every 2 cm. Each heater is periodically heated and by monitoring the thermal response, the medium in which the sensor is embedded in (air, snow, ice, water) can be identified.

WP3 : Atmospheric measurements

Arctic haze and aerosol layers frequently occur in the Arctic mid-troposphere from early spring to summer mostly due to anthropic perturbations. Other modifications due to natural and anthropic forcings are induced in cloud occurrence and properties. Such features are however not all easily detectable from space. Furthermore, ground-based observations are inexistent over most of the arctic. In this respect, we are developing at LATMOS in the frame of the project, an extension of the existing optical depth sensors (ODS) instrument and a fully new microlidar, to be operated as autonomous and unattended systems, to helpfully complement space observations. ODS is a sensor developed at LATMOS with the support of the CNES for the ESA/CNES Mars missions later cancelled. It is a double channel telescope of annular field of view equipped with silicium diode detectors, colour filter for selecting the wavelength, and an 8 decades amplifier allowing observations from the direct sunlight down to the very small moon scattered light. It is a light, small-sized and low consumption instrument fully qualified for space (TRL 5) and thus for low temperatures.

Currently, solid-state technology lidars (like ceilometers in airports) are the only instruments which have the potential to operate autonomously in a remote environment. However, we have to face a technical challenge to operate these systems in the harsh arctic environment where relatively small available power can be made available. The selected concept based on solid-state laser diodes is to be improved, so that the system is compacted and operated with an increased sensitivity and a capacity to discriminate water and ice phases in clouds. Acquisition and transmission of full-signal lidar waveforms and ODS data as a function of time is to be performed on a regular basis.

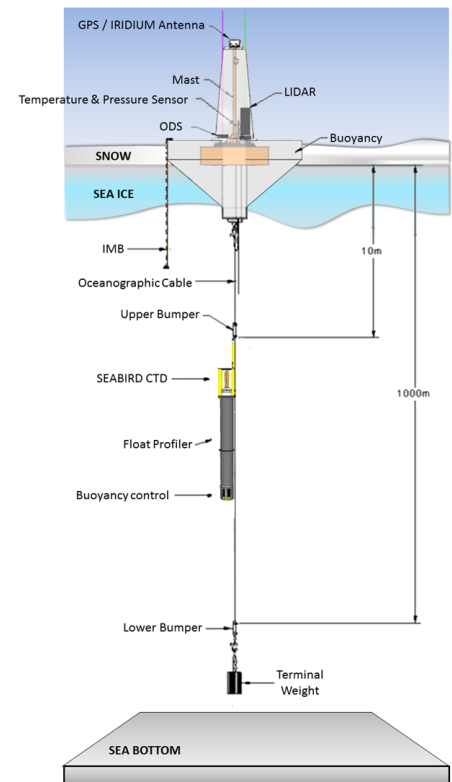


Figure 2 : IAOOS platform: profiling through the ocean, ice and atmosphere

Figure 2 : IAOOS platform: profiling through the ocean, ice and atmosphere. A synergy is being developed with work package 4 of NAOS (www.naos-equipex.fr) to deploy floats with biogeochemical sensors onto IAOOS platforms.

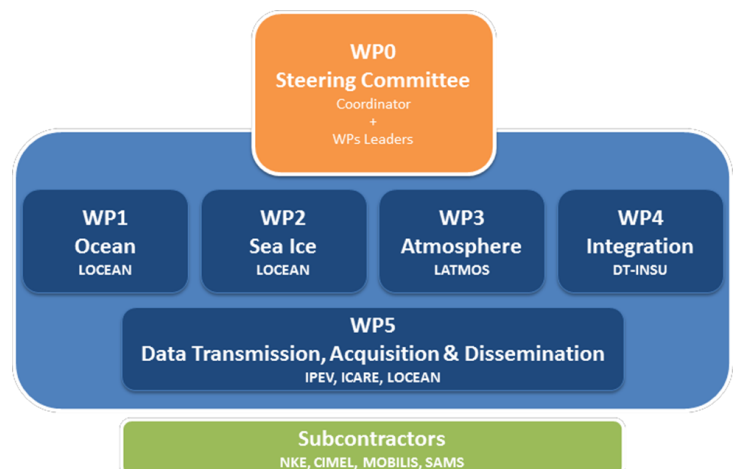


Figure 3 : Structure of the project

The selected concept based on solid-state laser diodes is to be improved, so that the system is compacted and operated with an increased sensitivity and a capacity to discriminate water and ice phases in clouds. Acquisition and transmission of full-signal lidar waveforms and ODS data as a function of time is to be performed on a regular basis.

WP4 : Integration

In the development phase, the accommodation of ODS and the microlidar onto the buoy is challenging due to the harsh atmospheric conditions of the arctic environment. In particular frosting and riming must be avoided on the optical windows. Tests in realistic meteorological conditions need to be performed.

The integration of the atmospheric sensors onto the buoy is placed under DT-INSU responsibility as well as the development of the atmospheric electronic systems on the buoy which gathers all the information from the various sensors, transmits them to satellite and receives order from land to modify the sampling strategy if necessary. Transmission is bidirectional so that the profiling rate and the acquisition rate can be modified as circumstances require.

In the operational phase, once the system has been developed and tested, all the elements will be gathered, controlled, assembled and tested before shipping in DT-INSU and IPEV in Brest. In this second phase, the activity in the facility in DT-INSU and IPEV in Brest thus comprises reception of the instruments from industrial providers and check proper functioning of all components (float, sensors, transmission, buoy..), integration, energy (lithium battery) packaging for the buoy, programming of the mission parameters (sampling strategy, compaction for transmission, ...), conditioning for transport and stock management.

WP5 : Data Transmission, Acquisition, Quality control and Dissemination

Each platform composed of three elements for oceanographic, sea-ice and atmospheric vertical profiles as described previously, will transmit data in near real time to a receiving station (IPEV, Brest, France) via satellites.

The data streams received from the IAOOS platforms through IRIDIUM will be retrieved and processed to level 0 by IPEV. Then the data will be sent to the GTS in the standard level 0 formats according to each data type. The oceanic data will then be retrieved from the GTS, processed and quality controlled both by the Coriolis data centre (www.coriolis.eu.org) and by the PIs of WP1. The sea-ice data will be retrieved from the GTS processed and quality controlled both by the IABP data centre (iabp.apl.washington.edu) and by the PIs of WP2. The atmospheric data will be retrieved from the GTS, processed and quality controlled both by the ICARE data center (www.icare.univ-lille1.fr/) and by the PIs of WP3. This double control is essential to guarantee a state of the art data validation.

The data centers are in charge of the dissemination through their usual systems. The data acquired in this project will thus be carefully validated and made publicly available and integrated in the international data bases. This way, after quality check and validation, the data will be distributed to the scientific community (ocean, sea-ice, atmosphere, climate communities), to operational and forecasting centers such as MERCATOR-Ocean (www.mercator-ocean.fr) and Meteo-France (climat.meteofrance.com/chgt_climat2).

A concomitant EU project lead by UPMC (PI J.C. Gascard) called ACCESS (Arctic Climate Change, Economy and Society, access-eu.org) will also contribute to the dissemination of IAOOS results. ACCESS is supported within the Ocean of Tomorrow call of the European Commission Seventh Framework Programme. Its main objective is to assess climatic change impacts on marine transportation (including tourism), fisheries, marine mammals and the extraction of oil and gas in the Arctic Ocean. ACCESS is also focusing on Arctic governance and strategic policy option.

Synthesis

The equipment to be built within IAOOS is unique and will allow partners to perform important technological and scientific breakthroughs. The technological developments performed for each WP will benefit the industrial SMEs involved and allow them to gain new markets.

The results aimed at are to get measurements from this network over at least three years with a representative regional coverage as initially planned. The novel, systematic and long term IAOOS array aims at a better understanding of environmental changes in the Arctic, at an improvement of the predictive capacity of how Arctic climate responds to a combination of natural and anthropogenic factors. Current climate models are unable to reproduce the recent changes observed in the Arctic environment. Sea ice is vanishing faster than in all coupled climate model scenario calculations. None of those calculations anticipated the 2007 drastic sea ice retreat. Models that feature sudden sea ice extent reductions put them later in the 21st century. To improve scenarios and climate models, a number of measures are necessary. In IAOOS, we will monitor the current status and changes of the Arctic sea ice to provide a baseline against which to compare projected future changes and to maintain the critical measurements that are needed to confirm and determine the trends in ocean, ice and atmospheric change.

AUTONOMOUSLY PROFILING THE NITRATE CONCENTRATIONS IN THE OCEAN: THE PRONUTS PROJECT.

By **F. D’Ortenzio**^(1,2), **S. Le Reste**⁽³⁾, **H. Lavigne**^(1,2), **F. Besson**^(1,2), **H. Claustre**^(1,2), **L. Coppola**^(1,2), **A. Dufour**^(1,2), **V. Dutreuil**⁽³⁾, **A. Laës-Huon**⁽³⁾, **E. Leymarie**^(1,2), **D. Malardé**⁽³⁾, **A. Mangin**⁽⁴⁾, **C. Migon**^(1,2), **P. Morin**^(5,6), **A. Poteau**^(1,2), **L. Prieur**^(1,2), **P. Raimbault**⁽⁷⁾, **P. Testor**⁽⁸⁾

¹ CNRS, UMR 7093, Laboratoire d’Océanographie de Villefranche, Villefranche sur-Mer, France

² Université Pierre et Marie Curie-Paris 6, UMR 7093, Laboratoire d’Océanographie de Villefranche, Villefranche-sur-Mer, France

³ IFREMER, Département Recherches et Développements Technologiques, Service Electronique, Informatique et Mesures in situ, Centre de Brest, BP 70, Plouzané, France

⁴ ACRI-ST, Sophia Antipolis, France

⁵ CNRS, UMR 7144, Chimie Marine, Adaptation et Diversité en Milieu Marin, Roscoff, France

⁶ Université Pierre et Marie Curie-Paris 6, UMR7144, Chimie Marine Adaptation et Diversité en Milieu Marin, Roscoff, France

⁷ Institut Méditerranéen d’Océanologie, OSU Pythéas, Marseille, France

⁸ Laboratoire d’Océanographie et du Climat: Expérimentation et Approches Numériques, Institut Pierre Simon Laplace, Université Pierre et Marie Curie, Centre National de la Recherche Scientifique, Paris, France

Introduction

In the 2000’s, a new optical sensor to evaluate nitrate (NO₃) concentration in seawater was realized (Johnson *et al.*, 2002) and then commercialized. Few years later, a first prototype of an APEX profiling float equipped with a NO₃ sensor was achieved and deployed in the Pacific Ocean, acquiring NO₃ profiles for about two years (Johnson *et al.*, 2010). The experiment with the APEX prototype indicated the huge potential of the duo “profiling float- NO₃ sensor” for a wide range of scientific applications, spanning from a better understanding of the physical biological interactions in the oceans (Claustre *et al.*, 2010) to a potential strongly enhancement of the performance of ecosystem models, via assimilation (Brasseur *et al.*, 2009).

In 2008, a large consortium of French laboratories dedicated a scientific and technological effort (PRONUTS project, GMMC + PACA region) to verify the feasibility of a PROVOR CTS03-based profiling float equipped with a NO₃ sensor (PRONUTS profiling float). The main aim was to develop two prototypes of PRONUTS, and to test their performances, in terms of sensor integration, of reliability of the couple profiling float+NO₃ sensor and of the quality of the collected data.

The PROVOR CTS03 series provides some unquestionable advantages. Its high reserve of floatability and large energetic autonomy could enable a large number of sensors, longer missions and improved cycling frequency. Moreover, a biogeochemical version (but without NO₃ sensor) of a PROVOR-based profiling float (PROVBIO) was already tested and scientifically exploited (Xing *et al.*, 2011); a new PROVBIO model, integrating an additional NO₃ sensor, could be then developed with few hardware and software modifications. This new PROVBIO model could provide simultaneous observations on the physical state of the water column (Temperature and Salinity profiles), on the chemical/resources distribution (NO₃ profiles) and on biological dynamics (Chlorophyll and Colored Dissolved Organic Matter profiles). This motivated to the PRONUTS project, which was strongly coordinated with the American and Canadian laboratories involved in the development of the APEX NO₃ profiling float (<http://www.mbari.org/chemsensor/APEXISUS.htm>).

In this note, we rapidly describe the technical characteristics of the two prototypes of PRONUTS that we developed. A short overview of the acquired profiles and of the (preliminary) data processing system will be done. Finally, some perspectives, in the framework of the NAOS-EQUIPEX and remOcean-ERC projects will be discussed.

The PRONUTS: a PROVOR-based NO₃ profiling float

Two NO₃ sensors were commercially available at the beginning of the project, both developed by Satlantic Inc: the SUNA and the ISUS sensors. The two instruments are based on the same principle: the measured absorption on the UV part of the spectrum permits to evaluate the NO₃ concentration, using the Beer-Lambert law. The SUNA sensor is the most recently developed device and the manufacturer suggested it as our primary choice. It is smaller and more compact than the ISUS, and, consequently, could be more easily integrated on a PROVOR. For the ISUS integration on an APEX, important hardware modifications were required (the instrument was squeezed and recombined in the interior of the APEX). A similar operation was required to mount an ISUS on a PROVOR, inevitably increasing technical difficulties and final costs. But since the ISUS has already been mounted on a profiling float (Johnson *et al.*, 2010), collecting data of very high quality, while no similar experiences existed on the SUNA, its development seemed important.

Both sensors are easily integrated with the PROVOR software, more specifically the version implemented on the PROVBIO. However, only the NO₃ concentration was transmitted on land, instead of the complete acquired absorption spectrum. This was the main difference with the APEX technical solution and the one having the greatest impact on the data quality. We will deserve a specific discussion in the next paragraphs.

After exchanges with our American and Canadian colleagues, and after some, preliminary tests, we decided to implement two versions of PRONUTS, the one equipped with a SUNA (PRONUTS-SUNA), the other with an ISUS (PRONUTS-ISUS). In the first case, the sensor was simply

connected to the PROVOR motherboard and externally installed on the side of the PROVOR tube (Figure 1, right). In the second case, the ISUS was entirely dismantled and then re-assembled into the PROVOR chassis, similarly to the APEX version (Figure 1, left).

All the preliminary tests (i.e. floatability, transmission, energy, on-board data processing) carried out on land or during some short deployments were successful for both versions. The two prototypes were ready to be deployed in May 2011.

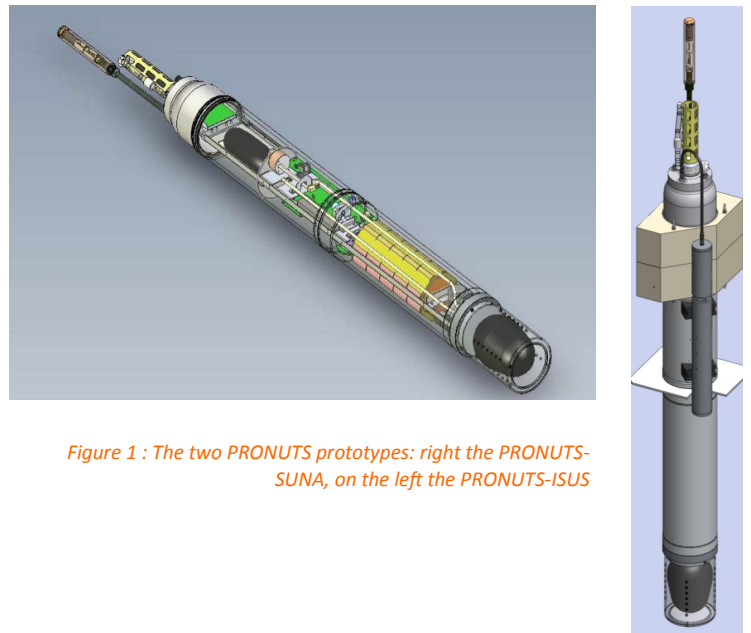
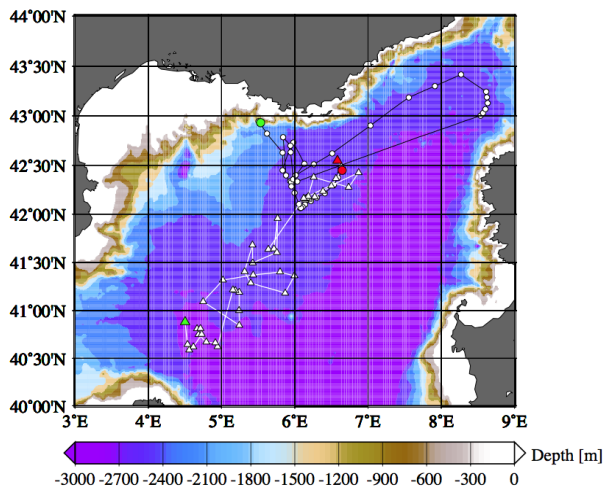


Figure 1 : The two PRONUTS prototypes: right the PRONUTS-SUNA, on the left the PRONUTS-ISUS

Figure 2 : Trajectories and positions of the profiles for the two PRONUTS in the North Western Mediterranean Sea. Triangles: PRONUTS-SUNA; Circles: PRONUTS-ISUS. Red dots indicate the deployment points (28 June 2011). Green dots indicate the last position at the moment of the writing of this note (end of February 2012).

The North Western Mediterranean Deployment

During the summer 2011, the two PRONUTS were deployed in the open North Western Mediterranean (Figure 2), in the framework of the Mediterranean Ocean Observing System for the Environment observing system (MOOSE) during the MOOSE-GE cruise (PI P. Testor). The area was selected for two main reasons:

- in a strong oligotrophic environment lasting for most of the year, winter deep water convection events, followed by huge phytoplankton blooms, are recurrently observed in the area (D'Ortenzio *et al.*, 2009); the range of variability of the NO_3 concentrations was supposed to be high, giving an ideal site to test the PRONUTS performance (Marty *et al.*, 2002);
- in the framework of the French MOOSE Mediterranean observing system (http://www.allenvi.fr/?page_id=777) the area is recurrently monitored by research vessels, which strongly facilitates any logistic issues during the PRONUTS tests (in case of failure, for example, a recover of the profiling floats could be easily planned).

The sampling strategy was strictly the same for the two PRONUTS, and it was fixed to be as close as possible to the strategy of the APEX NO_3 float. At 100 levels from 1000m depth (at 10 m resolution) to surface seven measurements were acquired in a very rapid sequence, and transmitted to land at the profiling float surfacing. Initial cycling frequency was based on the standard ARGO protocol (10 days), although sensor restrictions limited the maximum profiling depth to 1000m. Parking depth was set at 1000m.

Data processing was different from the APEX- NO_3 protocol (K. Johnson, personal com). For the APEX- NO_3 profiling float, the whole acquired spectrum (from 200 to 400 nm) was transmitted on land. The NO_3 concentrations were then derived by specific algorithms, which corrected eventual sensor bias or any interference in the UV absorption due to salinity and temperature effects (Sakamoto *et al.*, 2009). For the PRONUTS, the estimation of the NO_3 concentrations was carried out directly by the sensors, and no information on the spectrum were available on land. Consequently, the PRONUTS data could be likely affected by erroneous NO_3 estimations, which could not be corrected.

For this reason, a high-resolution profile of NO_3 concentrations by water samples analysis was carried out during the deployment, and a calibration of the first profiles was performed (Figure 3). For the following profiles, a preliminary calibration procedure was applied, based on two main hypotheses derived during the tests on land (Lavigne *et al.* in preparation). According to the first hypothesis, NO_3 concentration at depth is relatively stable all along an annual cycle. More specifically, we assume that the possible variations of the NO_3 concentration at depth are about the sensors accuracy ($\pm 2 \mu\text{mole}$). For each profile, and for the whole lifetime of the PRONUTS, a calibration factor was calculated by difference between the average of the PRONUTS data in the 800-1000 m layer and the deep values obtained at the deployment by water sample analysis. The second hypothesis is that the calibration factor could be linearly applied to the whole profile (i.e. possible bias of the sensors is linear).

Presently (February 2012) 43 NO_3 profiles of the PRONUTS-SUNA and 46 profiles of the PRONUTS-ISUS were collected (Figure 4) and validated (i.e. correct lat/lon position, complete profile). The PRONUTS-ISUS experienced a serious transmission failure in September, with a total loss of contact. Fortunately, the contact was re-established in November and, up to now, no other severe malfunctions were detected. The data of the PRONUTS-SUNA were generally more noisy than the data of the PRONUTS-ISUS (compare error bars on Figure 3).

For both sensors, the calibration method appears promising. After the application of the calibration factors, the surface values during the oligotrophic period (i.e. August to October) are close to zero, as expected in the area. NO_3 surface concentrations start to be significant when important events of mixed layer deepening bring nitrates from the deep reservoir to the surface through mixing (i.e. in December 2011, for the PRONUTS-SUNA, Figure 4). The event of mixed layer deepening observed by the PRONUTS-ISUS (> 1000m), which induced a complete homogenization of the NO_3 concentrations (Figure 4) is particularly spectacular. In order to better monitor the sequence of the mixed layer deepening and the modifications of the NO_3 concentration vertical structure, the frequency of cycling from both prototypes was switched to 2 days, starting from the 15th of January.

This mechanism of re-distribution of NO_3 along the water column after a deep mixing event is relatively a well known process, but was never quantified in-situ like that before to our knowledge.

Conclusions and Perspectives

At the present day (February 2012), the two PRONUTS are still operational, and the acquired data are visible in real-time on the web (<http://www.oao.obs-vlfr.fr/pronuts/pronuts.html>). Despite some technical problems (in particular on the PRONUTS-ISUS), both prototypes successfully carried out their mission. The calibration procedure, although not perfect, seems to accomplish the first-order scientific requirements (i.e. depths of nitraclines), and appears as a promising method when absorption spectrum data are not available. However, the strong mixing event observed by the PRONUTS-ISUS, modifying the NO_3 concentrations over the whole water column, could overrule our first calibration hypothesis. A first check of the quality of the method will be possible at the coming back of oligotrophic conditions (i.e. June, July), when surface NO_3 concentration values should be close to zero again. Alternatively, the recovery of the prototypes is considered. This operation, although always potentially risky, could allow to evaluate the degree of degradation of the two prototypes and of the sensors.

The experience and the know-how acquired during the PRONUTS project will be strongly capitalized in the next years. Two important funded projects (the NAOS EQUIPEX, PI PY LeTraon, <http://www.naos-equipex.fr/Le-Projet>, and the remOcean ERC Advanced Grant, PI H. Claustre, <http://www.oao.obs-vlfr.fr/projects/ongoing-large-projects>) plan to deploy more than 60 biogeochemical profiling floats in key areas of the world ocean (North Atlantic, Mediterranean, Arctic) during the period 2012-2015. The pool of the NAOS and remOcean biogeochemical profiling floats will partially include a new version of PROVBIO. This new version will be equipped with the “standard” PROVBIO sensors suite (CTD, backscatterometers, irradiance sensors, fluorometers for Chl and CDOM, optodes for oxygen) plus a NO_3 concentration sensor (most likely a SUNA).

No more PRONUTS will be produced. The two prototypes demonstrated the feasibility of the PROVOR based observations of NO_3 concentrations and the next step is now to couple such physical and chemical observations with biological ones.

Acknowledgments

The PRONUTS project is a program co-funded by the GMMC and by the PACA region (project “MOOSE-Radfloat”). The PABIM GMMC project (PI F. D’Ortenzio) also contributed to the PRONUTS experiment. We would like to thank the crew of the R/V Tethys II, used for the PRONUTS deployment phases. Many thanks also to Kenneth Johnson for its invaluable expertise on the ISUS and SUNA sensors and for the accurate answers to our hundreds and hundreds e-mails. Finally, we would like to thank the whole Coriolis group for the assistance in the PRONUTS preparation and in the data quality control.

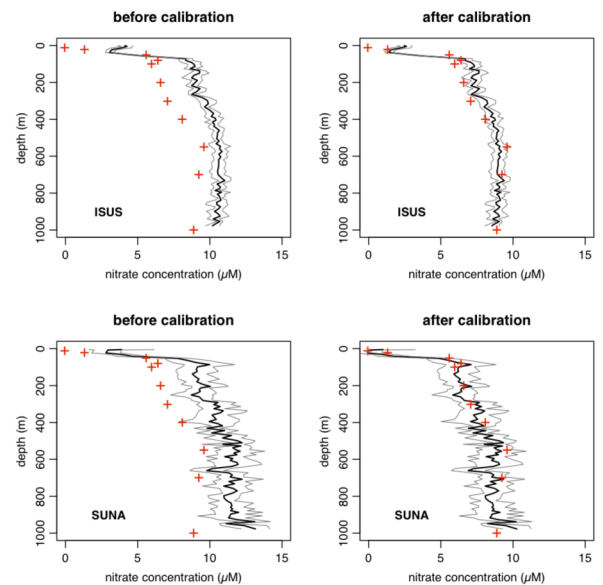


Figure 3 : First profiles of NO_3 concentration from the two PRONUTS prototypes (black lines) and the corresponding standard deviation (grey lines). Red crosses indicate the NO_3 estimations by water samples carried out at the deployment (28 June 2011). Upper panels: PRONUTS-ISUS ; lower panels : PRONUTS-SUNA. On the left : not calibrated NO_3 profiles ; right: calibrated profiles.

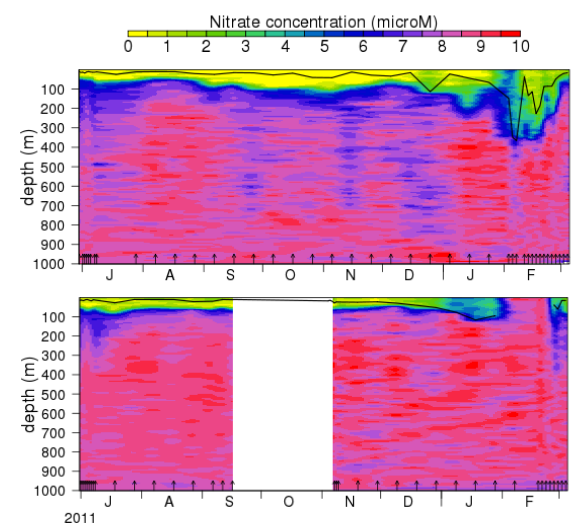


Figure 4 : Times series of the NO_3 concentration as a function of time and depth. Upper panel PRONUTS-SUNA ; lower panel PRONUTS-ISUS. The black lines indicate the mixed layer depth, estimated from T and S profiles of the floats. The arrows indicate the time of the profiles.

References

- Brasseur P, Gruber N, Barciela R, et al. (2009) Integrating Biogeochemistry and Ecology into Ocean Data Assimilation Systems *Oceanography*, 22, 26-30.
- Claustre H, Bishop J, Boss E, et al. (2010) Bio-optical profiling floats as new observational tools for biogeochemical and ecosystem studies. Proceedings of the "OceanObs, 09: Sustained Ocean Observations and Information for Society Conference", 2.
- D'Ortenzio F, d'Alcala MR (2009) On the trophic regimes of the Mediterranean Sea: a satellite analysis. *Biogeosciences*, 6, 139-148.
- Johnson KS, Coletti LJ (2002) In situ ultraviolet spectrophotometry for high resolution and long-term monitoring of nitrate, bromide and bisulfide in the ocean. *Deep-Sea Res. I*, 49, 1291-1305.
- Johnson KS, Riser SC, Karl DM (2010) Nitrate supply from deep to near-surface waters of the North Pacific subtropical gyre. *Nature*, 465, 1062-1065.
- Marty JC, Chiaverini J, Pizay MD, Avril B (2002) Seasonal and interannual dynamics of nutrients and phytoplankton pigments in the western Mediterranean Sea at the DYFAMED time-series station (1991–1999). *Deep Sea Research II*, 49, 1965–1985.
- Sakamoto CM, Johnson KS, Coletti LJ (2009) Improved algorithm for the computation of nitrate concentrations in seawater using an in situ ultraviolet spectrophotometer. *Limnology and Oceanography-Methods*, 7, 132-143.
- Xing X, Morel A, Claustre H, et al. (2011) Combined processing and mutual interpretation of radiometry and fluorimetry from autonomous profiling Bio-Argo floats: Chlorophyll a retrieval. *J. Geophys. Res*, 116, C06020.

EGO: TOWARDS A GLOBAL GLIDER INFRASTRUCTURE FOR THE BENEFIT OF MARINE RESEARCH AND OPERATIONAL OCEANOGRAPHY

By Pierre Testor^{1,2}, Laurent Mortier¹, Johannes Karstensen³, Elena Mauri⁴, Karen Heywood⁵, Dan Hayes⁶, Pekka Alenius⁷, Alberto Alvarez⁸, Carlos Barrera⁹, Laurent Beguery², Karim Bernardet², Laurent Bertino¹⁰, Agnieszka Beszczynska-Möller¹¹, Thierry Carval¹², Francois Counillon¹⁰, Estelle Dumont¹³, Gwyn Griffiths¹⁴, Peter M Haugan^{10,15}, Jan Kaiser⁴, Dimitris Kasis¹⁶, Gerd Krahnemann², Octavio Llinas⁹, Lucas Merckelbach¹⁷, Baptiste Mourre⁸, Kostas Nittis¹⁶, Reiner Onken¹⁷, Fabrizio D'Ortenzio¹, Sylvie Pouliquen¹², Alexander Proelss¹⁸, Rolf Riethmüller¹⁷, Simón Ruiz¹⁹, Toby Sherwin¹³, David Smeed¹⁴, Lars Stemmann¹, Kimmo Tikka⁶, Joaquin Tintoré¹⁹

¹ UPMC, Université Pierre-et-Marie-Curie, Paris, France

² CNRS, Centre National de la Recherche Scientifique, La Seyne/m, France

³ GEOMAR | Helmholtz Centre for Ocean Research, Kiel, Germany

⁴ OGS, Istituto Nazionale di Oceanografia e di Geofisica Sperimentale, Trieste, Italy

⁵ UEA, University of East Anglia, Norwich, United Kingdom

⁶ OC-UCY, University of Cyprus, Nicosia, Cyprus

⁷ FMI, the Finnish Meteorological Institute, Helsinki Finland

⁸ NURC, NATO Undersea Research Center, La Spezia, Italy

⁹ PLOCAN, Plataforma Oceanica de Canarias, Gran Canaria, Spain

¹⁰ NERSC, Nansen Environmental and Remote Sensing Center, Bergen, Norway

¹¹ AWI, Alfred Wegener Institute for Polar and Marine Research, Bremerhaven, Germany

¹² IFREMER, Institut Français de Recherche pour l'Exploitation de la Mer, Brest, France

¹³ SAMS, Scottish Association for Marine Science, Oban, United Kingdom

¹⁴ NOC, National Oceanography Centre, Southampton, United Kingdom

¹⁵ UIB, University of Bergen, Bergen, Norway

¹⁶ HCMR, Hellenic Centre for Marine Research

¹⁷ HZG, Helmholtz-Zentrum Geesthacht, Geesthacht, Germany

¹⁸ UT, Universität Trier, Trier, Germany

¹⁹ CSIC, Agencia Estatal Consejo Superior de Investigaciones Científicas

Background

The concept of underwater gliders emerged from the work of Douglas Webb in 1986. His scientist colleague Henry Stommel anticipated their development and their use. He wrote an impressive “science fiction” article which was published in *Oceanography* (Stommel, 1989). In looking back on Stommel’s article anticipating autonomous gliders, we can now marvel at how much of what followed he had predicted. In the 1990 s, while gliders were being developed and successfully passing first tests, their potential use for ocean research started to be discussed in international conferences because they could help us improve the cost-effectiveness, sampling, and distribution of the ocean observations (see OceanObs’99 Conference Statement – UNESCO). After the prototype phase, three different operational gliders (Figure 1) were presented by their designers in Davis et al. (2002) and applications to ocean research were highlighted in Rudnick et al. (2004). Later on, one could only witness the growing glider activity throughout the world.

In 2004, the first European glider experiments were carried out in the framework of the European project MFSTEP of the Fifth Framework Programme (FP5). Later, the European FP6 project MERSEA in 2006-2009 and several national past and on-going projects have supported many glider operations in European and foreign waters. The first glider experiments in Europe brought together several teams that were interested in the technology and a consortium formed naturally from these informal collaborations. This relatively small group then expanded as increasing numbers of institutions began investing in this technology. In 2006, yearly European Gliding Observatories (EGO) Workshops and Glider Schools were first organized, which attracted teams from outside Europe (Australia, Canada, Mexico, South Africa, USA), whilst also becoming the international forum for glider activities (<http://www.ego-network.org>). Because of the international interest, as well as the relevance to a number of stakeholders, EGO has now come to mean “Everyone’s Gliding Observatories.”



Figure 1: The three operational gliders (from left to right: Seaglider, Slocum, Spray) transferring, while at surface, the data they just collected underwater and receiving new commands thanks to the bidirectional link Iridium link.

The group discussions within EGO turned into a Community White Paper presenting the glider activity of the last 10 years and some prospects for the next 10 years for the observation of the global ocean, which was presented at the OceanObs'09 Conference in Venice (Testor et al. 2010). Impressive results have already resulted from the glider activity. Using various on-board sensors, gliders resolve a wide range of spatial and temporal scales and reveal an amazing number of oceanic features. Glider data help us to better understand and characterize the oceanic physical and biogeochemical variability at basin scale, mesoscale, and even submesoscale (from 10^3 km horizontally and 1 month to 1 km and 1 hour). There is now a general agreement that the further development of ocean observations with gliders is necessary to better understand the ocean because they are capable to provide sustained synoptic observations of wide area ocean regions. Moreover, the assimilation of glider data in global and/or regional/coastal numerical models can significantly reduce the uncertainties of our ocean state estimates (physical and biogeochemical) leading to more accurate "ocean products" that provide new research opportunities and economic applications (e.g. fish farming, oils spill detection and spreading) but also satisfy safety aspects (e.g. search and rescue, naval applications) and decision making.



Figure 2: EGO - COST Action ES0904 partner countries in the European area on 2012/02/21 (BE, CY, DE, FI, ES, FR, GR, IL, IR, IS, IT, NO, PL, PT, SE, UK), South Africa has already joined the Action, Australia, Canada, Egypt, Mexico, Tunisia and Turkey have expressed their intention to join.

Some key challenges have emerged from the expansion of the glider system and require now setting up a sustainable European as well as a global system to operate glider and to ensure a smooth and sustained link to the Global Ocean Observing System (GOOS). Glider technology faces many scientific, technological and logistical issues. In particular, it approaches the challenge of controlling many steerable probes in a variable environment for better sampling. It also needs the development of new formats and procedures in order to build glider observatories at a global level. Several geographically distributed teams of oceanographers now operate gliders, and there is a risk of fragmentation.

Our consortium intends to solve most of these issues through scientific and technological coordination and networking. This approach is supported by the ESF through Cooperation in the field of Scientific and Technical Research (COST). The **COST Action ES0904 "EGO"** started in July 2010 aiming to build international cooperation and capacities at the scientific, technological, and organizational levels, for sustained observations of the oceans with gliders. Yearly calls provide the opportunity to grant student exchanges, travel, meetings, training, and publications that are related to our glider activity (see <http://www.ego-cost.eu>). One major impact of the COST Action was the inception of several European countries to get involved in aspects related to underwater glider operations (Figure 2). Another major impact of this Action was the elaboration of the EU Collaborative Project **GROOM, Gliders for Research, Ocean Observation and Management** for the FP7 call "Capacities – Research Infrastructures", which addresses the topic "design studies for research infrastructures in all S&T fields" and its recent acceptance (see <http://www.groom-fp.eu>).

The GROOM project: A Design Study on a European Research Infrastructure for gliders

The GROOM project started in November 2011 and addresses more specifically the progress that can be achieved with gliders to improve the objectives, coverage, resolution and organization of existing marine observation systems. The overarching goal of GROOM is to assess the requirements and to provide a roadmap for the installation of a sustained and distributed glider component as part of a European Network of Marine Observatories and as such as a contribution to the GOOS. The European glider infrastructure should safely operate individual as well as fleets of gliders in order to create a continuum of observations. Operations shall be coordinated to fill the gaps left by present marine observation systems on global, regional and coastal scale, with benefits for both fundamental marine research and operational oceanography.

The GROOM objectives, as well as the assessment of its potential impacts, are mainly formulated in the context of the concepts, reference terms and calls raised by the instruments and roadmaps set up recently by the vision statement "Towards a European Network of Marine Observatories" of the Marine Board (MB) of the European Science Foundation and by the program Global Monitoring for Environment and Security (GMES). The MB highlighted that there is a crucial need for "a long term, stable and integrated network of strategic marine observatories, installed and operated through multinational cooperation and support, providing consistent in-situ data from the seas and oceans in support of the EU Integrated Maritime Policy and as a driver for smart, sustainable and inclusive growth in Europe (Europe 2020)". The GMES started to be reality, with the Marine Core Service (MCS), which was rapidly established in line with discussions within the Group for Earth Observation (GEO). The MyOcean programme started in 2009 and is now implementing the adequate and sustained framework for the integration of data needed for the 4D mapping of the state of the ocean to deliver marine services. As an important consequence, the need for reliable sustained observing system providing adequate *in situ* data for assimilation and validation started to increase. The GMES In-Situ Coordination (GISC) was established in 2010 by EEA as an FP7 programme. It is now the reference frame for the assessment of marine observation systems aiming at providing real-time (RT) data for the MCS and is drafting an ocean in situ observing system convenient to the MCS, based on terms of feasibility, costs and benefits.

The objectives for this design study for a European glider Research Infrastructure (RI) are to demonstrate that

- 1) A distributed architecture of “gliderports” around the European seas and overseas (see figure 2), working in close coordination, is the required and cost effective way to operate fleets of gliders in combination with the other existing observing systems,
- 2) This glider infrastructure is suitable to deploy, maintain and operate individual as well as fleets of gliders continuously for operational monitoring and research.
- 3) Such infrastructure can provide a world-class service to the research and environment monitoring communities.

The geographical distribution (Figure 3) is desirable in the sense that it multiplies the possibilities for servicing gliders and is in phase with the ROOS concept. However, it is potentially a weakness as the European glider engineering teams may not individually reach the critical size to be able to pilot gliders. The GROOM goal here is to foster the different initiatives from these different teams avoiding duplicate efforts. GROOM will help us to reach a stage where gliders can be used in numbers by the scientific and marine monitoring communities to contribute to the GOOS/ROOS. Through GROOM we will deploy gliders for dedicated process studies and creative applications and seek to avoid duplication of the efforts required by such a glider activity.

Significant progress could be achieved with such an RI for gliders appearing as a single entity based on land facilities in a number of distributed “gliderports”. This would improve:

- Scientific coordination of the European resources (how/where to deploy gliders? which sensors?),
- Technological coordination (to develop new platforms/sensors),
- Harmonisation of the procedures for glider deployments, piloting and recoveries,
- Definition of ownership and governance definition of rules for transnational access,
- Data access and dissemination with single-point portal and a data/metadata format which is compliant with international standards.



Figure 3: GOOS/ROOS considered in the MyOcean project (1) Global ocean, (2) Arctic Ocean (Arctic ROOS), (3) Baltic Sea (BOOS), (4) Atlantic European North West Shelf Ocean (NOOS), (5) Atlantic Iberian Biscay Irish Ocean (IBI-ROOS), (6) Mediterranean Sea (MOON and Med-GOOS), (7) Black Sea (Black Sea-GOOS) ; European possible “gliderports” are indicated by yellow stars.

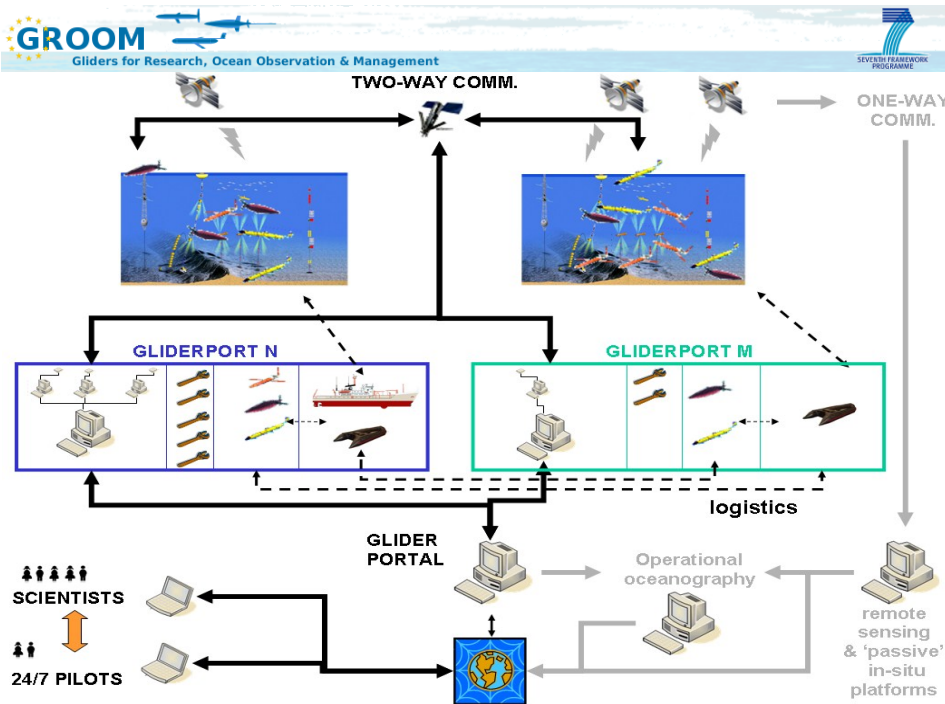


Figure 4: GROOM vision of integrating the two-way communication capabilities in the existing observing and modelling system. Scientists would interact with 24/7 pilots in order to steer the glider fleet in an optimised way, getting all relevant information on the marine environment (numerical products, remote sensing images, GIS, in-situ data from other platforms, etc.). This would be based on an infrastructure of several “gliderports” (from left to right: communication and computer resources, workshops for maintenance and development, pools of gliders, sea-access) distributed according to the GOOS/ROOS strategy.

A future European infrastructure for gliders will be defined in GROOM based on what exists and the existing, but fragmented, glider infrastructure. A network of gliderports could compose a distributed ground segment (Figure 4), which would have to be based on tight networking for computers and software, on efficient man-machine interfaces and tools from artificial intelligence, as well as on at-sea experience. A focus will be given to 1) the currently existing, distributed ground-segment, 2) the glider scientific payload technology, 3) the tools to plan/dimension the glider effort to be made in order to fulfil the scientific objectives defined by preparatory actions and 4) the costs of the individual Member State glider activity.

Such a structure to be designed by the GROOM project will have to stimulate and not stifle all the creative applications of the glider technology. Therefore, the innovative part in operating gliders for science will be explored. The use of new sensors and sensor combinations (synergy) on gliders to observe, in near real time, all the components of the marine environment, including ecosystems (and in particular in complex oceanic regions: fronts, sub-mesoscale features, under-ice observations) will be examined.

Another one of the main issues that GROOM has to address is to find the optimal topology for the gliders' sampling in relation with the gaps of the pre-existing networks (in-situ and satellites) and operational circulation models. Obviously, this depends on the objectives of the networks in terms of spatial and temporal resolution, the nature and variability of the parameters and processes to be monitored as well as on the estimate of the ocean state used for the decision. The design and execution of new missions will have to be carried out to guarantee that a successful implementation of the various infrastructure parts designed in GROOM is possible. At the same time, the GROOM project will trial new techniques and approaches that will be key features for the future ocean observing system.

Finally, the GROOM project aims also at assessing the possible governance of such a European glider observing system. The goal is certainly not an entity centralizing all European gliders, such as UNOLS for ships in the US or IMOS in Australia. A distributed version is preferred and in the long term, one can imagine that the different glider teams supported by the EU and national authorities might contribute with their resources to a European pool of gliders. Whether coordinated calls for proposals may be useful, also has to be discussed. This design study will first describe in detail why a governance structure would be required and investigate how it could be implemented.

Conclusions and perspectives

Sustained observations of the ocean are mandatory on a variety of space and time scales and gliders can certainly contribute to this, if deployed in combination with other existing ocean observing systems (research vessels, Ocean-Sites moorings, Argo profiling floats, XBTs, satellites, volunteer ships, surface drifters, radars, acoustic arrays, ...) according to science-driven objectives. The optimal configuration of the Research Infrastructure proposed by GROOM will have to be beneficial for both marine research and operational oceanography, being able to carry out both intense process studies and continuous monitoring. The gliders offer really new capabilities in terms of sampling and have a tremendous potential for the scientific payload, so we expect this project will lead to frontier-science studies that cut across platforms and types of ocean observations, and will develop synergies with projects contributing to the GOOS (like Euro-Argo, JERICO, FIXO3, ACOBAR ...) and the project MyOcean2 in the next coming years.

References

- Davis R., Eriksen C., and C. Jones, (2002): Autonomous buoyancy-driven underwater gliders, in *The Technology and Applications of Autonomous Underwater Vehicles*, G. Griffiths, ed., Taylor and Francis, London, 2002
- Rudnick D., Davis R., Eriksen C., Frantantoni D. and M.J. Perry, (2004) "Underwater Gliders for Ocean Research," *Marine Technology Journal*, vol. 38, no. 1, Dec., pp. 48-59, 2004.
- Stommel H. (1989) *The Slocum Mission*, *Oceanography*, April 1989
- Testor, P., Meyers, G., Pattiaratchi, C., Bachmayer, R., Hayes, D., Pouliquen, S., Petit de la Villeon, L., Carval, T., Ganachaud, A., Gourdeau, L., Mortier, L., Claustre, H., Taillandier, V., Lherminier, P., Terre, T., Visbeck, M., Krahman, G., Karstensen, J., Alvarez, A., Rixen, M., Poulain, P.M., Osterhus, S., Tintoré, J., Ruiz, S., Garau, B., Smeed, D., Griffiths, G., Merckelbach, L., Sherwin, T., Schmid, C., Barth, J.A., Schofield, O., Glenn, S., Kohut, J., Perry, M.J., Eriksen, C., Send, U., Davis, R., Rudnick, D., Sherman, J., Jones, C., Webb, D., Lee, C., Owens, B., Frantantoni, D., (2010): Gliders as a component of future observing systems, in *Proceedings of the "OceanObs'09: Sustained Ocean Observations and Information for Society" Conference (Vol. 2)*, Venice, Italy, 21-25 September 2009, Hall, J., Harrison D.E. and Stammer, D., Eds., ESA Publication WPP-306.

CIRENE: FROM CYCLONES TO INTERANNUAL TIMESCALES IN THE SOUTH-WESTERN TROPICAL INDIAN OCEAN

By **J. Vialard⁽¹⁾** (for the Cirene team), **Praveen Kumar B.⁽²⁾**, **N. C. Jourdain⁽³⁾**, and **M. Bador⁽⁴⁾**

⁽¹⁾ IRD, LOCEAN, Paris, France

⁽²⁾ CSIR, NIO, Goa, India

⁽³⁾ LEGI, CNRS-UJF, Grenoble, France (now at CCRC, UNSW, Sydney, Australia)

⁽⁴⁾ Currently at LEGOS, Toulouse, France

Why study the Indian Ocean?

There are 23 countries which gather the third of the world's population within and around the Indian Ocean (including the French island of La Réunion). A lot of these countries have emerging or developing economies, with fragile infrastructures, and a large proportion of the population whose livelihood depends on agriculture. This makes most of these countries vulnerable to weather and climate events. Fourteen of the twenty deadliest cyclones in the world history for example formed within the Bay of Bengal (Longshore 2008). The most recent dramatic example was cyclone Nargis that claimed 140 000 lives in Myanmar in 2008 (Webster 2008).

The Indian Ocean was once thought as a relatively passive ocean from a climate perspective, in comparison to the neighbouring Pacific Ocean that hosts the powerful El Niño phenomenon (McPhaden et al. 2006). But recent studies deeply changed this view. First, an intrinsic mode of interannual climate variability was discovered in the Indian Ocean, and given the (not very imaginative) name of Indian Ocean Dipole (IOD, Saji et al. 1999, Webster et al. 1999). Several studies suggest that this phenomenon strongly influences climate variability around the Indian Ocean (e.g. Yamagata et al. 2004), or the evolution of El Niño (e.g. Izumo et al. 2010). Second, the Madden-Julian oscillation (MJO), i.e. the main mode of atmospheric variability at intraseasonal timescale (Zhang 2005), initially develops in the tropical Indian Ocean, before propagating eastward and affecting tropical rainfall along its track. Several international field experiments supported by the Climate Variability (CLIVAR) World Meteorological Organization (WMO) program have hence been organized in the Indian Ocean after 2000 (MISMO, CIRENE, CYNDY/DYNAMO). The review paper by Schott et al. (2009) provides a detailed overview of the other numerous incentives to bring back the Indian Ocean on the front of the climate scene.

One region of particular interest in that context is the "Thermocline Ridge of the Indian Ocean" (TRIO). In this region (Figure 1a), the mean structure of the wind promotes Ekman pumping and lifts the thermocline, in particular during Austral summer. This shallow thermocline coexists with very high Sea Surface Temperatures, close to the threshold of deep atmospheric convection. This favours strong air-sea interactions at many timescales (see Vialard et al. 2009 for a review). This region is in particular a cyclogenesis region and Xie et al. (2002) hypothesised that interannual variations of the heat content there could influence the number of cyclones that hit La Réunion and/or Madagascar. This region also has one of the strongest Sea Surface Temperature (SST) responses to the MJO in the Tropics (Duvel and Vialard 2007). Finally, this region displays interannual SST anomalies associated with IOD and/or El Niño events, with clear climate impacts, for example on the following monsoon rainfall over west India (Izumo et al. 2008).

For all those reasons, the importance of studying the TRIO region was outlined by the international community (CLIVAR Indian Ocean Panel science plan, 2006). The Cirene cruise was part of this international effort to understand air-sea interactions at multiple time scales (cyclones, MJO, IOD) in the TRIO region. In the current newsletter, we will describe the Cirene program, its links with the Mercator and Coriolis projects. Section 2 describes the Cirene oceanographic cruise. Section 3 focus on the large interannual anomalies associated with the IOD captured by the Cirene, Coriolis and Mercator data. Section 4 describes the oceanic response to Dora cyclone, as captured by Cirene, and Mercator data. Section 5 provides several conclusions, from the Coriolis and Mercator programs perspective.

The Cirene oceanographic cruise

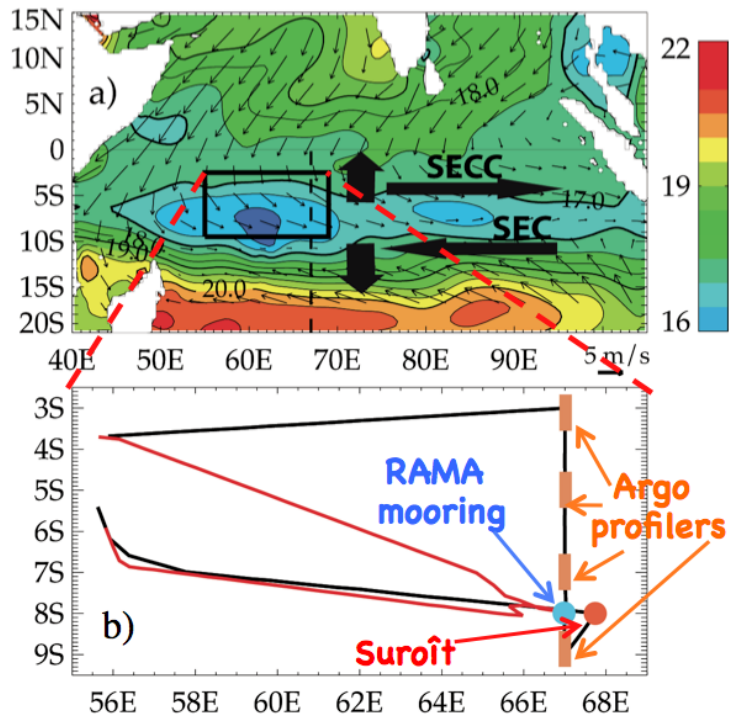
The main science goal of the Cirene oceanographic cruise was to describe air-sea interactions in the TRIO region. More specifically, Cirene did address the following timescales and questions. 1) What is the oceanic signature of the IOD in the TRIO region, and can we understand its mechanisms? 2) What are the processes responsible for the strong SST response to the MJO in this region? 3) Does the shallow thermocline in the TRIO region influence cyclogenesis and do interannual anomalies associated with the IOD influence cyclogenesis in this region?

Cirene was endorsed by the CLIVAR Indian Ocean and Asian-Australian Monsoon Panels (IOP and AAMP). Cirene was an element of the Coriolis contribution to the Argo program by deploying a total of 19 PROVOR profiling floats (9 in 2005 and 10 in 2007) within the TRIO region. Cirene also contributed to the international Research Moored Array for African-Asian-Australian Monsoon Analysis and Prediction (RAMA) program (McPhaden et al. 2009), with the deployment of the first flux reference site in the TRIO region in January 2007 and its maintenance in July 2008.

There is a two-way interaction between the Cirene and Mercator / Coriolis programs. Cirene contributes to Coriolis through instrument deployments (PROVOR profilers, XBT during the cruises) and to Mercator by analysis and re-analysis evaluation, as will be illustrated in this newsletter. In return, Coriolis and Cirene data products provided the necessary large-scale context in which to insert the Cirene data, allow-

ing for a richer data analysis and better understanding of processes. This two-way approach will be illustrated as often as possible in the current newsletter.

Figure 1. a) Average 0-300m temperature climatology in December-March from the WOA09 database (colors) with QuickScat December-March wind climatology as vectors. The TRIO region is roughly outlined by the black frame. In this region, the wind-driven Ekman flow (schematized by thick black arrows) results in a shallow thermocline. The South Equatorial Counter Current (SECC) lies on the northern flank of the thermocline ridge, and the South Equatorial Current (SEC) on its southern flank. b) Zoom of the black frame in a. The Suroît track (with XBT deployments every 30 miles) is indicated in black (1st leg) and red (2nd leg). PROVOR profilers deployment sites are indicated in orange. The 8°S, 67°E RAMA mooring is indicated by a blue circle and the long Suroît station 30 miles further east by an orange circle



Cirene was the oceanographic part of the Vasco-Cirene project. The Vasco project focussed on cyclogenesis and air-sea interactions associated with the MJO; and was based on surface layer balloon (Aeroclippers) deployments from the Seychelles (Duvel et al. 2009). The synchronous Cirene cruise, on board Ifremer (Institut Français de Recherche pour l'Exploitation de la Mer) R/V Le Suroît was organized in two legs, in January and February 2007. The cruise started, made a port call and returned to Victoria in Seychelles. The first leg track is indicated in black on figure 1b, and the second leg is indicated in red. Expandable bathythermographs provided by the Coriolis program were deployed every 30 miles along both legs (figure 1b). A north-south section across the thermocline ridge was performed at 67°E. PROVOR profilers provided by the Coriolis program were deployed at 3°S (3 profilers), 5°S (3 profilers), 7°S (3 profilers) and 9°S (1 profiler, figure 1b). The groups of 3 profilers were deployed with standard Argo profiling characteristics (e.g. one profile every 10 days, 1000m parking depth, 0-2000m profiles), but were programmed to profile every third alternate-day, hence providing an increased temporal resolution during the first few months after the cruise. A mooring was deployed at 8°S, 67°E as part of the RAMA program. Most of the cruise consisted of a long station at 8°S, 67° 30'E, with intense air-sea fluxes, and high-frequency ocean profiles sampling (refer to Vialard et al. 2009 for a more detailed description of the cruise).

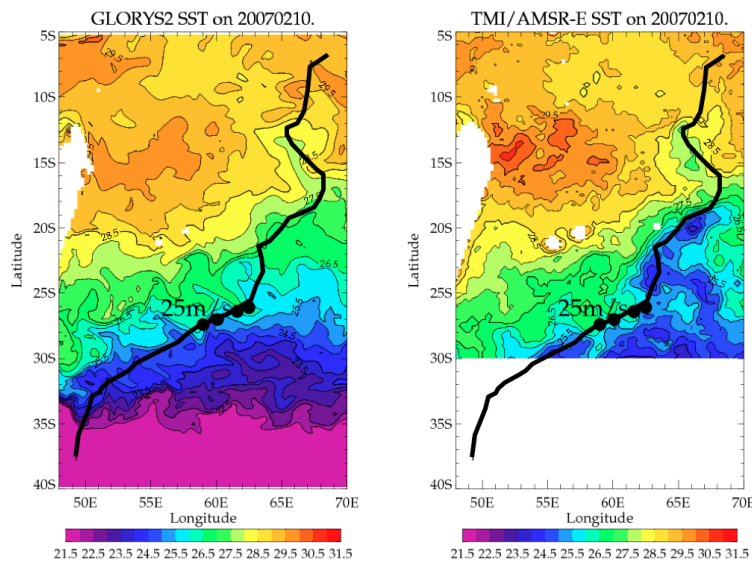


Figure 2. (Left) GLORYS2 SST analysis on the 10th February 2007. (Right) TMI-AMSR-E microwave SST estimates on the same date. The full track of the Dora cyclone is indicated by the black line. The recorded positions of the cyclones on that day are indicated by black disk (the average cyclone maximum winds on that day was 25 m s^{-1}).

The cruise science objectives were to monitor cyclones, the MJO and the oceanic signature of the IOD. We were lucky with two of those three objectives during the cruise itself. A strong IOD event occurred in late 2006, and generated strong thermocline depth anomalies in the eastern half of the Indian Ocean, between 5°S and 12°S. By the time of the cruise, these anomalies had propagated westward as planetary waves and we monitored the vertical structure in the region of largest sea level interannual anomalies (Vialard et al. 2009). The whole duration of the Cirene cruise was associated with inactive MJO, but the instruments deployed during the cruise (RAMA mooring, Argo profilers) allowed to monitor and analyse the processes of a very strong MJO event in late 2007 (see conclusions).

On January 27 2011, a tropical disturbance formed almost exactly over the mooring and Suroît location. The system was upgraded to a moderate tropical storm named Dora on January 29. Dora meandered southward (see Figure 2 for the Dora track) over the next two days while strengthening, and Météo-France upgraded it to a tropical cyclone early on February 1. Dora reached its strongest intensity (930 hPa and 190 km/h winds) on February 3, at about 15°S and remained intense until the 9th. The Vasco-Cirene program provided unique observations of both the oceanic response to the storm (Le Vaillant et

al. 2012) in a region of strong air-sea interactions, and of surface winds in the storm eye wall from Aeroclippers further south (Duvel et al. 2009).

In the next two sections, we will focus on describing the ocean signature of the IOD and then of the Dora cyclone, from a combination of Cirene and Coriolis data, and from the Mercator GLORYS2 re-analysis.

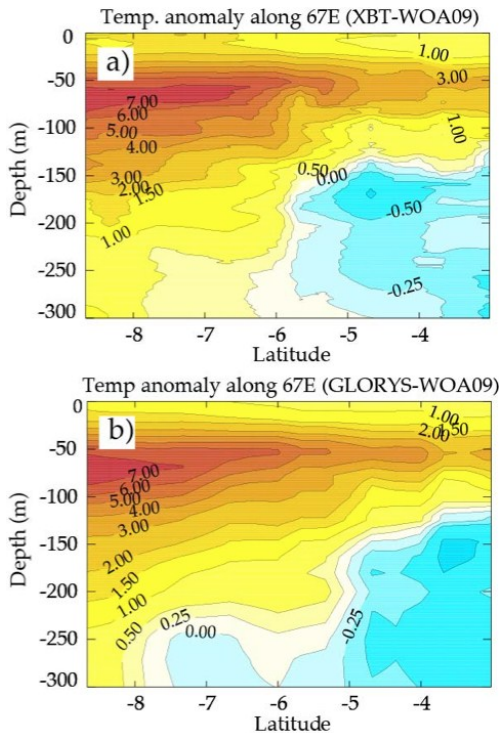
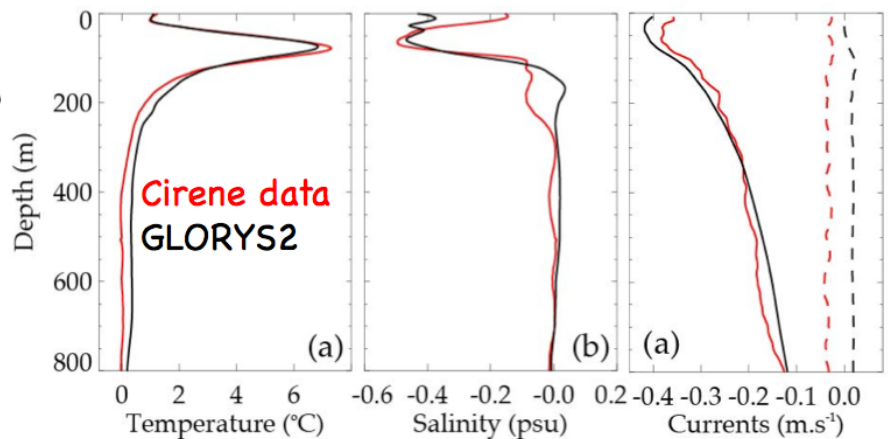


Figure 3. Latitude-depth section of temperature interannual anomalies along the Cirene section at 67°E from a) Cirene XBT measurements and b) GLORYS2 re-analysis. The WOA09 climatology is used in both cases to compute interannual anomalies.

Figure 4. Average oceanic profiles at 8°S, 67°30'E during January-February 2007 (Cirene data in red and GLORYS2 re-analysis in black). a) Temperature and b) Salinity anomalies with respect to the WOA09 climatology. c) Zonal (continuous line) and meridional (dashed line) current.



Sampling the Indian Ocean Dipole

In the past there had been little observations in the TRIO region in general, and no in situ salinity and currents measurements of the IOD signature in particular (Vialard et al. 2009). Figure 3 shows a meridional section of the temperature anomaly through the TRIO at 67°E from the Coriolis-sponsored XBT section (3a) and from the Mercator GLORYS2 re-analysis (3b). Both capture the very clear warm anomaly in the thermocline. The basic mechanisms of those thermocline depth anomalies is already known in the TRIO region, from the study of Masumoto and Meyers (1998) study: Ekman pumping associated with the IOD easterly anomalies in winter drive mass convergence between 5°S and 10°S in the eastern and Central Indian ocean, which then propagates westward as planetary waves.

But Cirene also provided a one-month salinity and currents profiles record at that point from conductivity-temperature-depth (CTD) and lowered Acoustic Doppler Current Profiler (ADCP) measurements from the Suroît (Figure 4). This figure shows that the upper 100m were anomalously fresh by 0.2 to 0.5 psu at the same location (Figure 4b). It also shows relatively strong westward currents down to 800 m, in a transition region between the South Equatorial Counter Current (SECC) and South Equatorial Current (SEC). This scientific objective interacted with Coriolis and Mercator objectives in two ways, illustrated here. First, the Cirene CTD and L-ADCP data has been retained from operational databases so far, so that figure 4 provides a real test for the performance of the GLORYS2 re-analysis. If the agreement of the Cirene and GLORYS2 thermal profile is not surprising (the XBT section of figure 3 was assimilated), the general agreement of the salinity anomalies profile is more convincing (GLORYS2 is only constrained by neighbouring Argo profiles). But the best demonstration of the quality of the GLORYS2 analysis in this region is the agreement of the currents profiles (currents are only constrained indirectly via multivariate constraints in the data assimilation and by the ocean model). Now that the good performance of GLORYS2 in this region has been established, it will be possible to use it in the future to reach our scientific goals. The CORA data, an objective analysis of Argo data produced by Coriolis, provides another way to restore the local Cirene observations in their large scale context. Figure 5 shows that there is a clear separation between fresh water from the eastern Indian Ocean and saltier water to the west. More detailed budget analysis (Praveen Kumar et al. in prep) show that westward displacements of this region are driven by zonal advection, while the sudden salt increase that happens every year at mid-year is linked to southward advection by the annual average Ekman flow. This provides an explanation of the salinity anomalies in figure 4b: the anomalous westward currents observed during Cirene (figure 4c) pushed fresh water more than usually (figure 5), resulting in a fresh anomaly at the Cirene location.

Oceanic response to the Dora cyclone

As we discussed earlier, the Dora tropical disturbance formed almost exactly at the Cirene site location, and later travelled south. Cyclones tend to cool the ocean surface along their track: the cyclone “cold wake”. The Dora cold wake is obvious on figure 2b, from TMI-AMSRE sur-

face temperature observations. For intense cyclones like Dora, and close to the cyclone track, most of the cyclone-induced cooling is due to intense vertical mixing (e.g. Vincent et al. 2012a for a recent and global quantification of that effect). Air-sea fluxes (enhanced turbulent fluxes and diminished shortwave) play in comparison a much smaller role. Theoretical and observational studies (e.g. Emanuel 1999, Cione and Ullhorn 2003) both indicate that the cold wake provides a strong negative feedback to the cyclone development by limiting evaporation that “feeds” the cyclone heat engine. They estimate that a 1°C cooling can reduce the cyclone intensity by ~40%. This is a strong incentive to study air-sea interactions under tropical cyclones in shallow thermocline regions such as the TRIO region. In the case of Dora, we are particularly interested in estimating whether the anomalously deep thermocline associated with the IOD favoured Dora intensification.

Figure 2 provides an evaluation of the oceanic response to Dora in the GLORYS2 re-analysis. The cold wake is obviously strongly underestimated in GLORYS2 (compare figure 2a and 2b, to the east of the track between 20 and 30°S). Cooling under tropical cyclones is strongly driven by mixing, and hence by the wind speed (and the cyclone displacement speed as well, but we won't discuss this here). Figure 6 shows a comparison of the maximum Dora wind speed in the GLORYS2 atmospheric forcing (blue), direct measurements along one Aeroclipper track (red), and the maximum wind speed from the IBTrACS cyclone database (Knapp et al. 2010, thick black line). It is obvious that the GLORYS2 forcing, that comes from the ERAinterim re-analysis (that has a 79 km horizontal resolution) strongly underestimates the maximum winds associated with the cyclone, and hence, the oceanic response. In the recent years (i.e. the scatterometer era), the root mean square error of maximum winds from 3-hourly ERA-interim to IBTRACS data is indeed 9 m/s for tropical cyclones ($17 < V_{mx} < 33$ m/s), and 28 m/s for stronger hurricanes (Jourdain et al. 2012). The GLORYS re-analysis suffers from the same problems, indicating that the higher resolution ECMWF operational winds (25 km during Cirene, 16 km since January 2010) used to force it do not resolve cyclones much better. In addition, assimilation of satellite SST in GLORYS is not sufficient to correct such brief and intense cooling events: it only corrects 1/3 of the cold wake underestimation in GLORYS (Jourdain et al. 2012).

Conclusions

We have not discussed results associated with the MJO response in this newsletter. They also illustrate the Cirene philosophy (i.e., the combination of a process study with longer terms observing systems) quite well. There was no active MJO during Cirene, but a strong event in late 2007. The RAMA mooring deployed during Cirene allowed us to analyse mechanisms of the SST signature of the MJO, and to conclude that air-sea heat fluxes were the dominating process (Vialard et al. 2008). In that study, the improved Argo profilers coverage in the TRIO region that resulted from Cirene-deployed Coriolis providers, allowed to compensate for missing data at the mooring location, and to reach our scientific objectives. In the other science questions that we investigated in the current newsletter, we also promoted interactions between multiple data sources. Cirene for example contributed to instrument deployments for Coriolis, and helps validating the Mercator GLORYS2 re-analysis. But in return, Mercator and Coriolis data products help us answering our science questions, in particular at the MJO and IOD timescales.

We will finish this paper with a couple of recommendations. First, Mercator analyses are now of sufficient quality to help us answering some of our science questions. A lot of these questions in oceanography ultimately resolve in trying to explain why the temperature, or currents changed a way or another. A very useful tool for that are the various physical terms of the heat, salt and momentum equations computed from the ocean model. Those outputs are currently not available for Mercator re-analyses, but should be made available for scientific use in the future. In a data assimilation context, the source/sinks terms associated with the assimilation increments should of course be made available along with the other physical terms.

Our second conclusion (and recommendation) is that the ocean response to cyclones is not well accounted for in the Mercator analyses and re-analyses. This is largely due to a strong underestimation of cyclone maximum winds in the ECMWF forcing products. Of course, this may not be a problem for cyclone intensity forecast purposes in which the key question is to provide a good estimate of the oceanic state ahead of the cyclone (Vincent et al. 2012b). But the effects of a cyclone take more than one month before being dissipated (Vincent et al. 2012a), and a bad accounting of those hence also affects the ocean analysis well after the cyclone passage. It is difficult to propose a good solution in an operational context, but we suggest that the approach of Vincent et al. (2012ab) could be followed in future Mercator re-analyses. In this approach, the cyclone strong winds along observed cyclone tracks from the IBTrACS database are specified using an analytical model fitted to observations (Willoughby et al. 2006). Vincent et al. (2012ab) show that this results in a good agreement between the TMI-AMSRE and modelled cold wake.

Acknowledgements

The contributors to the Cirene project are too numerous to be all included as co-authors, but we would like to thank here a few of the people with the most significant scientific contribution to this project: J-P. Duvel, M. McPhaden, P. Bouruet-Aubertot, Y. Cuippers, B. Ward, C. de Boyer Montégut, C. Menkes, S. Kennan, E. Vincent, G. Samson, S. Masson, G. Madec.

References

Cione, J. J., and E. W. Ullhorn (2003), Sea surface temperature variability in hurricanes: Implications with respect to intensity change, *Mon. Wea. Rev.*, **131**, 1783–1796.

- CLIVAR Indian Ocean Panel, 2006: The Indian Ocean Implementation Plan for Sustained Observations: Understanding the role of the Indian Ocean in the climate system, available from http://eprints.soton.ac.uk/20357/01/IOP_Impl_Plan.pdf
- Duvel, J-P. and J. Vialard, 2007, Indo-Pacific Sea Surface Temperature Perturbations Associated with Intraseasonal Oscillations of the Tropical Convection, *Journal of Climate*, **20**, 3056-3082.
- Duvel, J-P., C. Basdevant, H. Bellenger, G. Reverdin, A. Vargas and J. Vialard, 2009, The Aeroclipper: A New Device to Explore Convective Systems and Cyclones, *Bull. Am. Met. Soc.*, **90**, 63-71.
- Emanuel, K. A. (1999), Thermodynamic control of hurricane intensity. *Nature*, **401**, 665–669.
- Izumo, T., C. de Boyer Montégut, J-J. Luo, S.K. Behera, S. Masson and T. Yamagata, 2008: The role of the western Arabian Sea upwelling in Indian monsoon rainfall variability, *J. Climate*, **21**, 5603-5623.
- Izumo, T., J. Vialard, M. Lengaigne, C. de Boyer Montégut, S. K. Behera, J-J. Luo, S. Cravatte, S. Masson, and T. Yamagata, 2010 : Influence of the Indian Ocean Dipole on following year's El Niño, *Nature Geo.*, **3 (3)**, 168-172.
- Jourdain, N.C., Vialard, J., Barnier, B., Ferry, N. and Parent, L. (2012). Impact of atmospheric forcing versus data assimilation in two ocean reanalysis: ocean response to tropical cyclones. *In preparation*
- Knapp, K. R., M. C. Kruk, D. H. Levinson, H. J. Diamond, and C. J. Neumann, (2010), The International Best Track Archive for Climate Stewardship (IBTrACS): Unifying Tropical Cyclone Data, *Bull. Amer. Meteor. Soc.*, **10**.
- Le Vaillant, X., Y. Cuyppers, P. Bouruet-Aubertot, J. Vialard, M. McPhaden, 2012: Tropical storm-induced near inertial internal waves during the Cirene experiment: energy fluxes and impact on vertical mixing, *J. Geophys. Res.*, **in revision**.
- Longshore, D. (2008), *Encyclopedia of Hurricanes, Typhoons, and Cyclones*. Checkmark, 468 pp.
- Masumoto, Y. and G. Meyers, 1998: Forced Rossby waves in the southern tropical Indian Ocean, *J. Geophys. Res. (Oceans)*, **103**, 27589-27602.
- McPhaden, M. J., S. E. Zebiak, Sand, M.H. Glantz, 2006: ENSO as an integrating concept in Earth science. *Science*, 314, 1740-1745.
- McPhaden, M. J., G. Meyers, K. Ando, Y. Masumoto, V. S. N. Murty, M. Ravichandran, F. Syamsudin, J. Vialard, W. Yu, L. Wu, 2009: RAMA: Research Moored Array for African-Asian-Australian Monsoon Analysis and Prediction. *Bull. Am. Met. Soc.*, **90**, 459-480.
- Praveen Kumar, B., J. Vialard, M. Lengaigne, V.S.N. Murty, G. Foltz, M. McPhaden, and K. Gopala Reddy, Processes of interannual mixed layer temperature variability in the thermocline ridge of the Indian Ocean, *Clim. Dyn.*, **in prep**.
- Saji, N. H., B. N. Goswami, P. N. Vinayachandran and T. Yamagata, 1999: A dipole mode in the tropical Indian Ocean. *Nature*, **401**, 360-363.
- Schott, F. A., S.-P. Xie, and J. P. McCreary Jr., 2009, Indian Ocean circulation and climate variability, *Rev. Geophys.*, **47**, doi:10.1029/2007RG000245.
- Vialard, J., G. Foltz, M. McPhaden, J-P. Duvel and C. de Boyer Montégut, 2008, Strong Indian Ocean sea surface temperature signals associated with the Madden-Julian Oscillation in late 2007 and early 2008, *Geophys. Res. Lett.*, **35**, L19608, doi:10.1029/2008GL035238.
- Vialard, J., J-P. Duvel, M. McPhaden, P. Bouruet-Aubertot, B. Ward, E. Key, D. Bourras, R. Weller, P. Minnett, A. Weill, C. Cassou, L. Eymard, T. Fristedt, C. Basdevant, Y. Dandoneau, O. Duteil, T. Izumo, C. de Boyer Montégut, S. Masson, F. Marsac, C. Menkes, S. Kennan, 2009, Cirene: Air Sea Interactions in the Seychelles-Chagos thermocline ridge region, *Bull. Am. Met. Soc.*, **90**, 45-61.
- Vincent, E., M., M. Lengaigne, G. Madec, J. Vialard, G. Samson, N. Jourdain, C. E. Menkes and S. Jullien, 2012a: Processes setting the characteristics of sea surface cooling induced by Tropical Cyclones, *J. Geophys. Res.*, **accepted**.
- Vincent, E., M., M. Lengaigne, J. Vialard, G. Madec, N. Jourdain, and S. Masson, 2012b: Assessing the oceanic control on the amplitude of sea surface cooling induced by Tropical Cyclones, *J. Geophys. Res.*, **in revision**.
- Webster, P. J. (2008) Myanmar's deadly "daffodil." *Nat. Geosci.*, **1**, 488–490.
- Webster, P. J., A. M. Moore, J. P. Loschnigg, and R. R. Leben, 1999: Coupled oceanic–atmospheric dynamics in the Indian Ocean during 1997–98. *Nature*, **401**, 356–360.
- Willoughby, H. E., R. W. R. Darling, and M. E. Rahn (2006), Parametric representation of the primary hurricane vortex. Part II: A new family of sectionally continuous profiles, *Mon. Wea. Rev.*, **134**, 1102–1120.
- Xie, S.-P., H. Annamalai, F.A. Schott and J.P. McCreary, 2002: Structure and mechanisms of south Indian climate variability, *J. Climate*, **9**, 840-858.
- Yamagata, T., S. K. Behera, J.-J. Luo, S. Masson, M. Jury, and S. A. Rao, 2004: Coupled ocean-atmosphere variability in the tropical Indian

USE OF ARGO FLOATS TO STUDY THE OCEAN DYNAMICS SOUTH OF AFRICA: WHAT WE HAVE LEARNED FROM THE GOODHOPE PROJECT AND WHAT WE PLAN WITHIN THE SAMOC INTERNATIONAL PROGRAMME.

By Sabrina Speich⁽¹⁾, Michel Arhan⁽¹⁾, Emanuela Rusciano⁽¹⁾, Vincent Faure^{(1)*}, Michel Ollitrault⁽¹⁾, Annaïg Prigent⁽¹⁾, Sebastiaan Swart⁽²⁾

⁽¹⁾Laboratoire d'Océanographie Physique, Brest, France

⁽²⁾CSIR - Southern Ocean Carbon & Climate Observatory, Rosebank, South Africa

*Now at: Japan Agency for Marine-Earth Science and Technology (JAMSTEC), Kanagawa, Japan |

Introduction

South of Africa, the Southern Ocean provides the export channel for NADW to the global ocean and the passage for heat and salt from the Indian and Pacific oceans (Figure 1). This region is influenced by the largest turbulence observed in the ocean. The eastward flowing ACC, the South Atlantic Current and NADW meet with the westward flow of Indian waters carried by the Agulhas Current, leading to water masses exchanges through jets, meanders, vortices, and filaments interactions. These local mesoscale and submesoscale interactions and the derived meridional fluxes might constitute the major link between the Southern Ocean and the global meridional overturning circulation (MOC). At the same time, mixing and air-sea interactions are responsible for significant water masses properties modifications. Mounting evidence from palaeoceanographic and modelling studies suggest that interocean exchanges south of Africa are drivers of global climate change. For example, through their southern influence on the Atlantic portion of the OC, changes in the flux of warm, salty waters from the Indian Ocean may have triggered the end of ice ages, as well as effecting shorter-term climate variability. Yet, owing to the relative isolation of the region from the US and Europe, few modern observations time series existed in this sector of the global ocean before 2004. This was the main reason to foster an international cooperation to monitor regularly this oceanic sector.

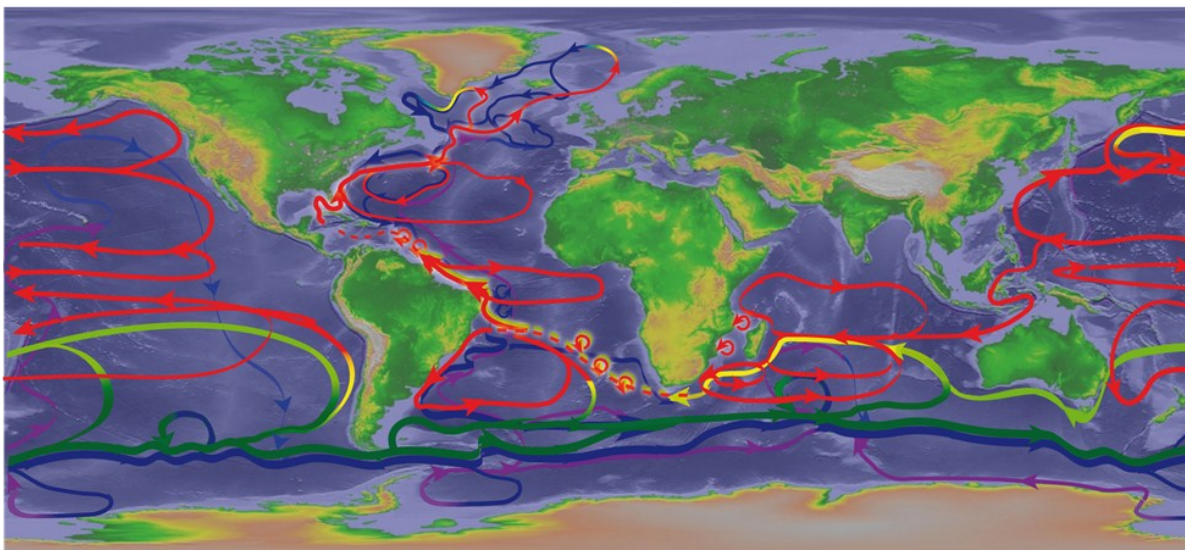


Figure 1. Schematic of the world ocean overturning circulation. Red is surface flows, blue and purple are deep flows, and yellows and greens represent transitions between depths. Base map derived by S. Speich, adapted from R. Lumpkin. This map is based on Speich et al., 2007, Blanke et al. 2001, and Lumpkin and Speer, 2007.

The project has been named GoodHope (GH hereafter) by the Cape of Good Hope. The international partnership is gathering together means (in terms of human, observing platforms, ship time and general financial support) from 11 different institutions and six countries (France, South Africa, United States, Germany, Russia and Spain). The project is coordinated by the *Laboratoire de Physique des Océans*, Brest, France. It has been approved in 2003 by the International CLIVAR panel and endorsed by SCAR and CLIC.

The GH experiment includes conductivity–temperature–depth (CTD) measurements (five realizations performed by the Shirshov Institute of Moscow, and a French multidisciplinary one, BONUS-GoodHope, achieved in early 2008 in the framework of the International Polar Year), geochemical tracer samplings, and expendable bathythermograph (XBT) measurements on the same and separate cruises. A large portion of the GH section was designed to follow a groundtrack of the JASON satellite, with the aim of joining hydrographic and altimetric data analyses

(Figure 2). ARGO floats launched during these cruises furthermore provide year-round hydrographic information on the region. A first description of water masses and full depth transport observations along the GH transect in late 2004 can be found in Gladyshev et al. (2008). Since it starts, GH has been one of the major projects in improving the data coverage of the Southern Ocean in terms of number of available monthly profiles.

With the relatively important number of full-depth hydrographic cruises, of high resolution XBT sampling, of deployed profiling floats and satellite altimetry in complement with numerical simulation analyses we have been able to improve quantitatively the knowledge on regional dynamics and water properties exchanged south of Africa. In particular the increased number of vertical profiles obtained by the repeat deployment of Argo floats along the GH line allowed us to make important progresses on the understanding and quantifying particular aspects of the regional dynamics. They include the estimate of the ACC variability for the upper 2500 m (Swart et al. 2010; Swart and Speich 2010; the regional mixing layer heat budget (Faure et al. 2010); aspects of the regional mesoscale dynamics (Gladyshev et al. 2008; Dencausse et al. 2011; Arhan et al. 2011); the Indo-Atlantic Antarctic Intermediate Water (AAIW) exchanges (Rusciano et al. 2012); global estimates of halothermohaline variability in connection with sea-level changes (von Schukman et al. 2012).

Hereafter we describe some of the results we obtained that are based, at least partially, on analyses of Argo data within the GH project.

Antarctic Circumpolar Current Variability

By using the entire *in situ* GH data set (full-depth hydrography and Argo data) we developed a proxy method based on the technique originally developed by Sun and Watts (2001 and 2002) and Watts et al. (2001) for the SO to project hydrographic sections onto a baroclinic stream function coordinate $\Gamma(\pi, \phi)$ (in this case dynamic height at the sea surface, referenced to a common pressure, ϕ_{2500}) in order to give us insight into the subsurface thermohaline structure of the ACC. This projection is called the gravest empirical mode (GEM). In particular, we combined the GEM with satellite altimetry SSH data and demonstrated the ability of this method to recreate *in situ* observations (Swart et al. 2010; Swart and Speich, 2010). This method provides us with a valuable 16 year time series (weekly intervals) of temperature and salinity fields at the GH line, which can be used to improve our understanding of the ocean dynamics in this least understood “choke point” of the ACC. Altimetry GEM (AGEM) is the name we assigned to this product. For the first time, the AGEM is able to provide information on the subsurface baroclinic structure of the ocean at eddy resolving spatial and temporal scales.

The continuous time series of thermohaline fields are, for example, exploited to understand the dynamic nature of the ACC fronts in the region. In particular, we derived weekly estimates of heat content (HC) and salt content (SC) for the ACC along GH (Figure 3). These estimates compare favorably to observed data. The resulting 16-year time series of HC and SC estimates are used to explain the subsurface thermoha-

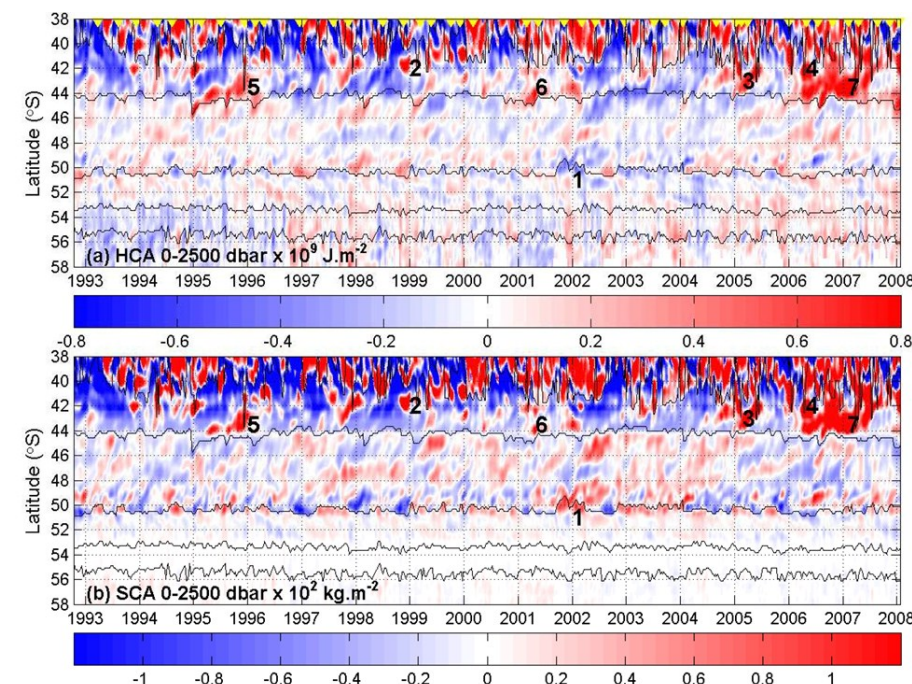


Figure 3. A Hovmöller representation of the (a) HCA and (b) SCA between the surface and 2500 dbar, along the GH line, from 1992-2008. The latitudinal positions of the ACC fronts (thin black lines) are from north to south: STF, SAF, APF, SACCF, SBdy. Adapted from Swart and Speich (2010).

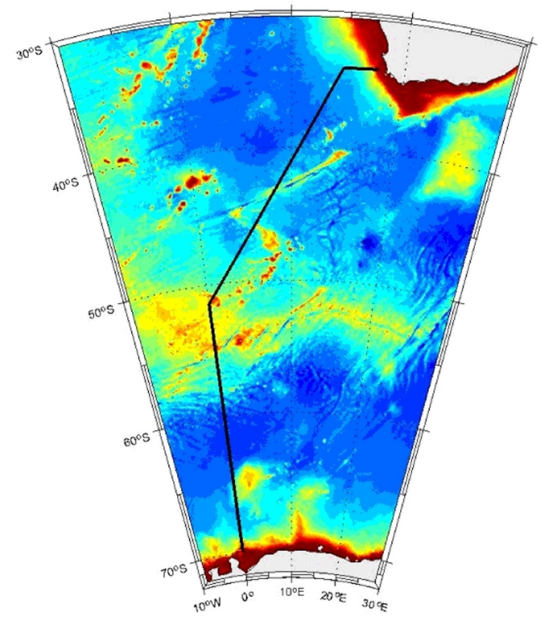


Figure 2. Locations of the GoodHope CTD and XBT sections.

line variability at each ACC front and frontal zone. The variability at the Subantarctic Zone (SAZ) is principally driven by the presence of Agulhas Rings, which occur in this region approximately 2.7 times per annum and are responsible for the longest and highest scales of observed variability.

The variability of the SAZ is responsible for over 50% and 60% of the total ACC HC and SC variability, respectively. Poleward of the SAZ, the variability is largely determined by the influence of the local topography on the fronts of the region and can be explained by the conservation of potential vorticity. Wavelet analysis is conducted on the time series of meridionally integrated HC and SC in each ACC front and frontal zone, revealing a consistent seasonal mode that becomes more dominant towards the south of the ACC. The lower frequency signals are compared with two dominant modes of variability in the Southern Ocean. The Southern Annular Mode correlates well with the HC and SC anomaly estimates at the Antarctic Polar Front, while the Southern Oscillation Index appears to have connections to the variability found in the very southern domains of the ACC.

Mixing Layer Heat Budget

While the oceanic region located south of South Africa has been studied extensively for its dynamical processes contributing to the transfer of Indian Ocean Central Water to the South Atlantic, other issues related to air-sea fluxes and water mass conversion, though also influencing the inter-oceanic exchanges, have been comparatively less examined in this area than at other longitudes of the Southern Ocean. A reason for this certainly resides in the fact that no Subantarctic Mode Water (SAMW) is formed in the SAZ south of Africa, unlike in the Indian Ocean and Pacific Ocean (McCartney, 1977; Sallée et al., 2008).

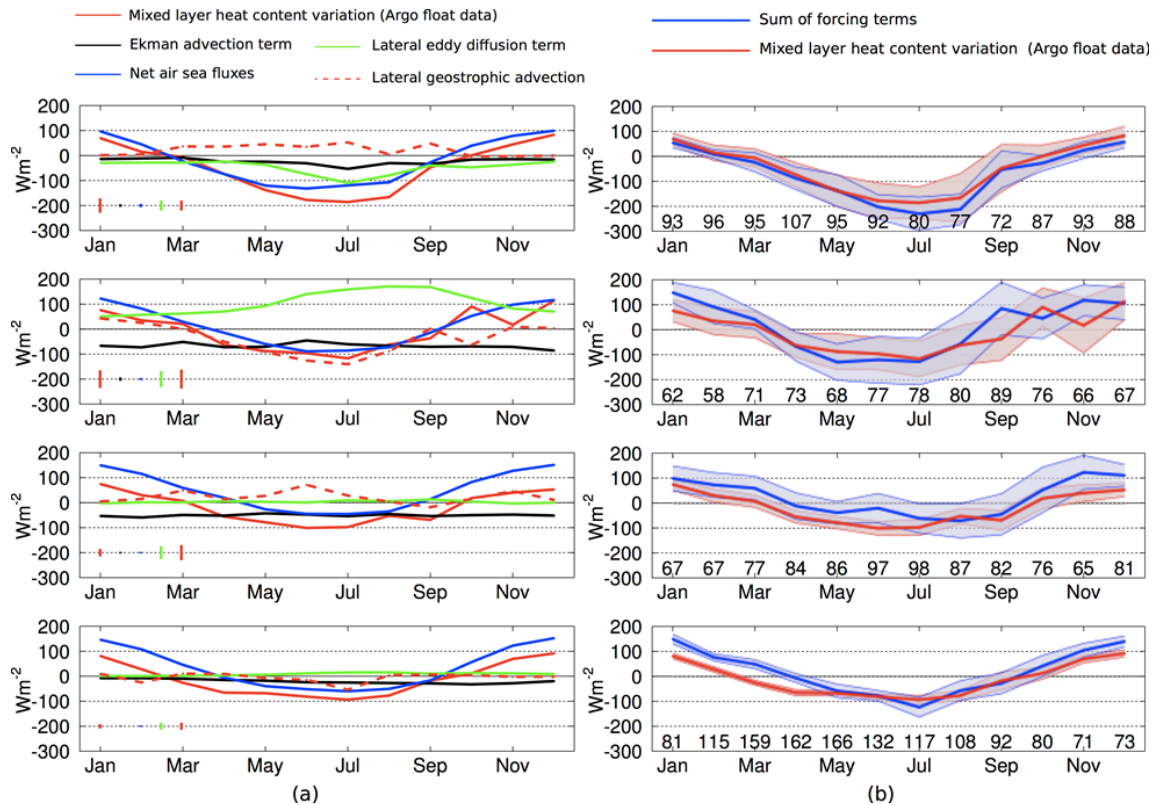


Figure 4. Seasonal variations of the SML heat budget terms of equation (1), averaged over the period 2004–2008. (a) The SML heat rate of change (left hand side of equation (1)) is shown along with each forcing term. (b) The heat rate of change is shown along with the sum of the forcing terms. Uncertainties were computed assuming that the number of independent individual heat budget estimates was one fifth of the number of ARGO profiles each month. Adapted from Faure et al. 2011.

In this study we used ARGO hydrographic profiles, two hydrographic GH transects, and satellite measurements of air-sea exchange parameters to characterize the properties and seasonal heat budget variations of the Surface Mixed Layer (SML) south of Africa (Faure et al. 2011). Two recent studies using ARGO floats, though not focused on the region south of Africa, provide information on the SML heat balance in this sector of the Southern Ocean. Sallée et al. (2006), while studying the formation of SAMW in the southeastern Indian Ocean, found that upstream (west) of this formation area heating by eddy diffusion related to the nearby South Indian western boundary current system (the Agulhas Current and Agulhas Return Current) counterbalances the cooling due to air-sea fluxes and Ekman transport. Dong et al. (2007), in a circumpolar study of the Southern Ocean SML heat budget, underlined the role of air-sea fluxes at the seasonal time scale, and the relative weakness of the geostrophic advection term, in contrast with western boundary current regions.

The analysis distinguishes the Subtropical domain (STZ), and the SAZ, Polar Frontal Zone (PFZ) and Antarctic Zone (AZ) of the ACC. While no Subantarctic Mode Water forms in that region, occurrences of deep SML (up to ~450 m) are observed in the SAZ in anticyclones detached from the Agulhas Current retroflexion or Agulhas Return Current. These are present latitudinally throughout the SAZ, but preferentially at longitudes 10°E-20°E where, according to Dencausse et al. 2011, the S-STF is interrupted. Likely owing to this exchange window and to transfers at the SAF also enhanced by the anticyclones, the SAZ shows a wide range of properties largely encroaching upon those of the neighbouring domains (Fig. 4).

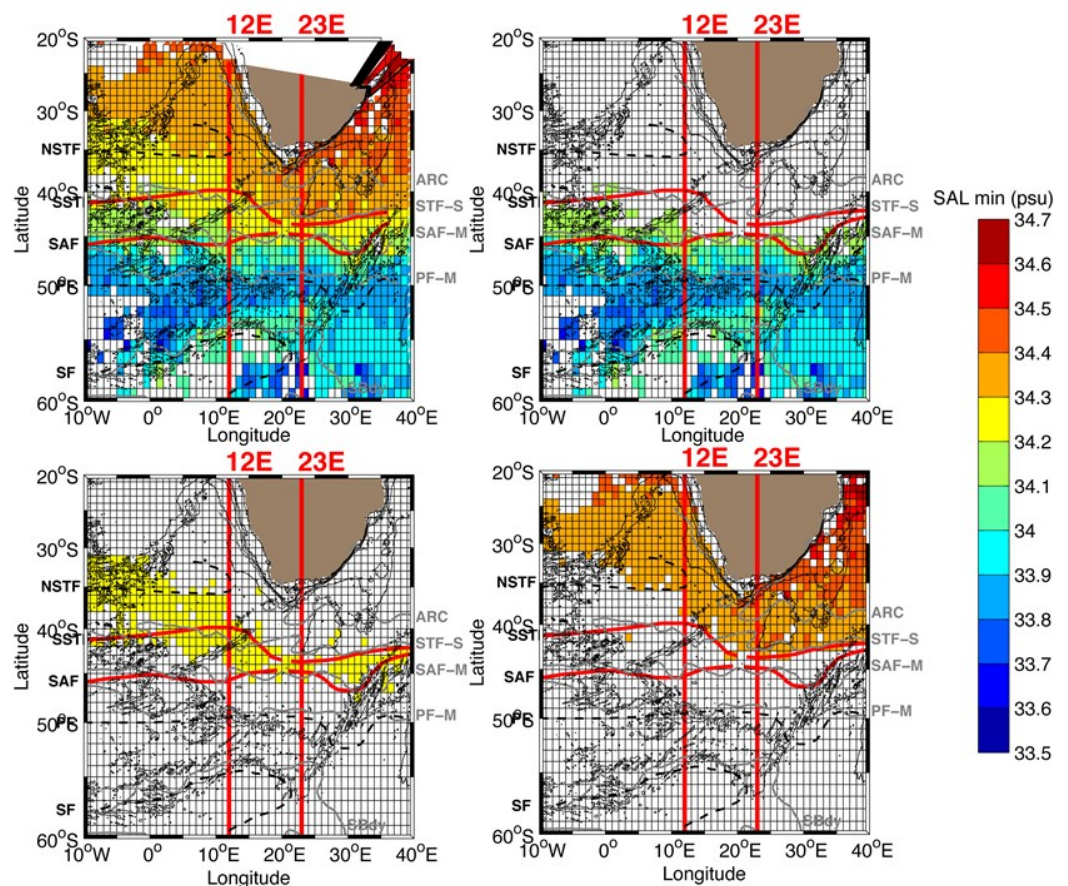
Heat budget computations in each zone reveal significant meridional changes of regime. While air-sea heat fluxes dictate the heat budget seasonal variability everywhere, heat is mostly brought through lateral geostrophic advection by the Agulhas Current in the STZ, through lateral diffusion in the SAZ, and through air-sea fluxes in the PFZ and AZ. The cooling contributions are by Ekman advection everywhere, lateral diffusion in the STZ (also favoured by the ~10-degree breach in the Subtropical Front), and by geostrophic advection in the SAZ. The latter likely reflects eastward draining of water warmed through mixing of the subtropical eddies.

Interocean Exchanges of Antarctic Intermediate Water

Here again we combined the ARGO hydrographic profiles collected between 2004-2009 in the South Atlantic south of Africa in combination with the a GH hydrographic transect to describe the characteristic and the flow of the Antarctic Intermediate Water (AAIW).

We reorganized the ARGO raw data in a 1° x 1° grid in an area extending from 10°W to 40°E and from 20°S to 60°S. The AAIW characteristics and dynamics are compared in nine (9) different regions defined on the base of the regional SO front that are relevant to the AAIW dynamics: the S-STF, and the SAF. Following Faure et al. (2010), the fronts location we used is the mean position of fronts defined as function of their surface dynamic height value and computed from the ARGO floats. We present here estimates of the relative importance of the different regional varieties of AAIW and their origins: south-west Atlantic (A-AAIW), characterized by salinities lower than 34.2, Indian (I-AAIW), with salinities exceeding 34.3, and a new intermediate water found north of the S-STF between 10°W and 12°E and south of the S-STF between 12°E and 40°E with salinities comprised between 34.2 and 34.3. We defined this water as Indo-Atlantic AAIW (IA-AAIW).

Figure 5. Salinity vertical minimum maps from Argo floats data. The subplots show S_{min} (top-left panel); $S \leq 34.2$ (top-right panel); $34.2 < S < 34.3$ (bottom-left panel); $S \geq 34.3$ (bottom right panel). Adapted from Rusciano et al. 2012.



The collected Argo profiles show a quasi-zonal distribution of the salinity minimum values computed within AAIW on the isoneutral surfaces ($\sigma^n = 27.3$) on a grid 1°x1°. The zonal AAIW matches fairly well the SO fronts location. The Indian and Atlantic varieties of AAIW are separated by the S-STF in the western part of the domain; the area to the north of the S-STF is largely dominated by I-AAIW with area-normalized volume values of about $5,14 \cdot 10^2 \text{ m}^3/\text{m}^2$, west of 23°E. The A-AAIW volume, abundant between the S-STF and SAF, decrease very importantly

eastward of 12°E certainly due to the mixing between Indian and Atlantic varieties because of the spawning of eddies in the Cape Basin that induces a strong mixing. This mixing has been measured in the SAZ south of Africa during the Bonus-GoodHope cruise. In the core of an anticyclone, the salinity minimum related with AAIW is 34.25, slightly above the values of the neighbouring stations. This salinity minimum is typical of the new water mass with intermediate characteristics between A-AAIW and I-AAIW.

Making use of the recently developed ANDRO velocity dataset (Ollitrault and Rannou, 2011) we estimate for the regional AAIW absolute geostrophic velocity and transport within the isoneutral layer. The AAIW has speed between 0.1 - 0.3 m/s in the Agulhas Current and 0.1 - 0.23 m/s in the Agulhas Return Current. AAIW flows in the subtropical region have a speed approximately of 0.03 m/s. A net increase of the eastward transport is evident from 40°S to 60°S, in particular at the S-STF and PF location. The transport across the latitudinal lines shows an evident variability between 12°E - 23°E, which represents the frontal “window” characterized by high mesoscale and submesoscale activity due to eddies and rings detected from in-situ observations and satellite altimetry.

Toward a South Atlantic observing network for the MOC (SAMOC)

The South Atlantic Ocean is not merely a passive conduit for remotely formed water masses, rather, within the South Atlantic Ocean, these water masses are significantly altered by local air-sea interactions and diapycnal fluxes, particularly in regions of intense mesoscale activity (Stramma and England, 1999; Sloyan and Rintoul, 2000). The importance of these contributions to the MOC has been highlighted by paleoclimate studies linking changes in the basin exchanges to abrupt climate changes (Duplessy and Shackleton, 1985; Weijer *et al.*, 2002; Peeters *et al.*, 2004; Rickaby and Bard, 2009).

Despite considerable effort and expenditure being deployed in the South Atlantic Ocean (see Figure 6 for a summary of ongoing/planned observations), the current range of observations being made are not capable of monitoring the OC, nor do they constitute a sustained observing system capable of monitoring large-scale interbasin fluxes of heat, freshwater, mass and other climate-relevant quantities.

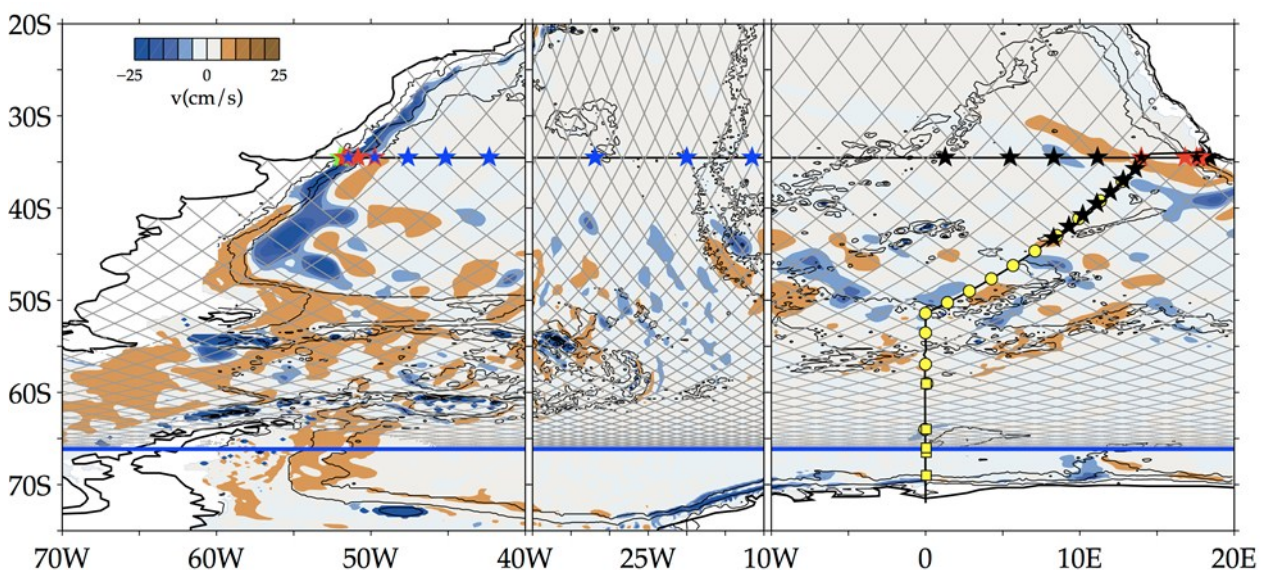


Figure 6. Schematic of the proposed trans-basin array along 34.5°S and the oblique GoodHope transect. Note the x-axis scale is stretched over western and eastern boundaries. Stars indicate the different components of the array that have been (or will be) submitted to respective funding agencies: eastern boundary PIES/CPIES by France-ANR (black stars), and western boundary bottom pressure gauges, CPIES and ADCP by Brazil-/FAPESP/FACEPE (green stars) dynamic height moorings to USA-NSF (red stars), western boundary PIES/CPIES and interior PIES-DP to USA-NOAA (blue stars). Colour contours are of 27-year mean OGCM For the Earth Simulator (OFES) meridional velocity at 200 m depth. JASON ground-tracks are overlaid as light gray lines.

Individual efforts to document the circulation in portions of its natural chokepoints (Drake Passage and South of Africa) are ongoing. Nonetheless, no proper quantitative monitoring system is in place, nor were these systems designed for long-term monitoring purposes. These are the reasons that brought a group of scientists to create a working group to foster collaborations and to discuss the design and implementation of an observational system to monitor the South Atlantic’s branch of the Meridional Overturning Circulation (SAMOC).

In the last five years, four workshops have been organized to achieve this objective. Copies of the presentations that were made at the workshops and complete workshops reports were published in Clivar Exchanges and are available on the NOAA-AOML web site at www.aoml.noaa.gov/phod/SAMOC/.

Following these meetings, and in particular the last one (the Fourth SAMOC Meeting, Simmon’s Town, South Africa, 27-30 September 2011), a coordination effort has been designed to implement the SAMOC observing network together with modelling and theoretical studies. International agreements for the use of resources from countries at the margins, or cruising the South Atlantic were made during the Infrastruc-

ture session. In particular, ships from Argentina, Brazil, Russia and South Africa are made tentatively available for the program.

Data from existing observational systems are crucial for the SAMOC field program. These include ARGO float deployment and the high-density XBT transects along 34.5°S (AX18), across Drake Passage (AX22) and south of South Africa (AX25). In particular, for the integrated observing platform we are building within SAMOC, it is really capital to maintain the homogeneity of the ocean sampling distribution in the region south of Africa as it is for today (this sampling has been obtained essentially *via* the ARGO float GoodHope programme : Figure 7). Others global observing systems, as the global drifter array, along with satellite observations of sea height, sea-surface temperature, sea-surface salinity (SMOS, and Aquarius) and surface wind will provide horizontal context for the SAMOC field program, as well as, information about the surface forcing. The SAMOC consortium constitutes an unprecedented opportunity to coordinate ship time with additional float deployments in the Southern Atlantic sector.

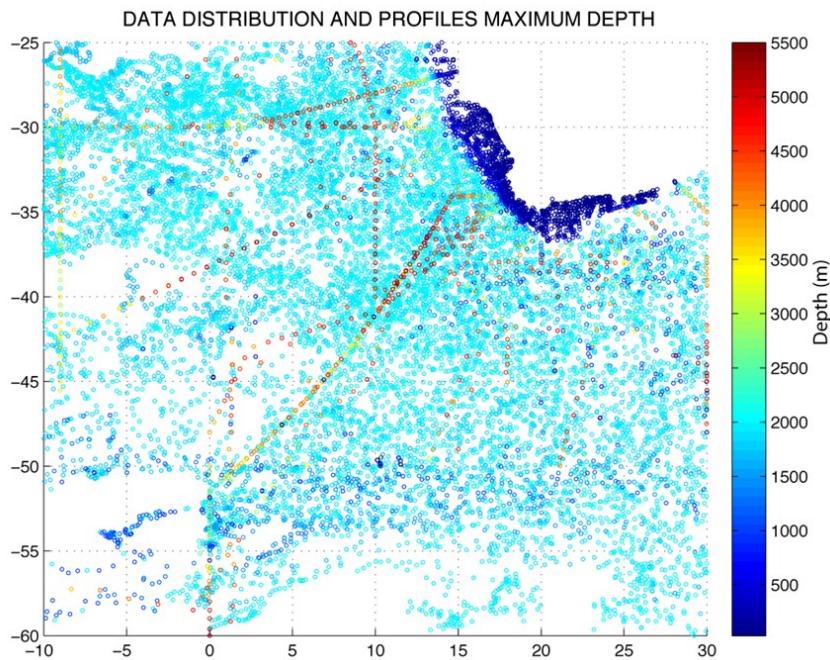


Figure 7. Distribution of hydrological observations in the region around south Africa and the Goodhope transect. Dots represent individual profiles from CTD casts and ARGO floats. Colours represent the maximum depth reached by each profile. From the figure it appears clearly that the sampling of ARGO floats (light blue dots) has completely changed, by improving it, the spatial coverage of hydrologic data in the region that was mainly based on deep hydrological transects (orange dots because they reach depths down to 5000 m).

Conclusions

The scientific interest of the ARGO network in the Southern Ocean is now accepted as evidence. Since the first deployment of profiling floats in this region in late 2003/early 2004, the GoodHope project effort has contributed significantly to SO unfolding. With the establishment of this network we have now access to the surface and subsurface structure of the ocean and their seasonal to interannual variations. This has enabled us to progress in a very fast and quantitative way on the knowledge of the specific ocean dynamics of the SO.

Aknowledgments

The IPY/BONUS-GoodHope and CLIVAR/GoodHope projects received support, in France, from the Institut National des Sciences de l'Univers (INSU), the CNRS, the IFREMER program "Circulation Océanique", and the Agence Nationale de la Recherche (ANR). the Groupe Mission Mercator Coriolis. The SAMOC project is funded in France by the ANR, Ifremer, UBO-IUEM.

References

- Ansorge, I., S. Speich, J. Lutjeharms, G. Goni, H. Rautenbach, W. Froneman, S. Garzoli, and M. Arhan, 2004: Monitoring the oceanic flow between Africa and Antarctica : Report of the first GoodHope cruise. *J. of African Science*.
- Arhan, M., S. Speich, C. Messenger, G. Dencausse, R. A. Fine, and M. Boye, 2011: Anticyclonic and cyclonic eddies of subtropical origin in the subantarctic zone south of Africa, *J. Geophys. Res.*, doi:10.1029/2011JC007140
- Blanke, B., S. Speich, G. Madec, et K. Döös, 2001 : A global diagnostic of interocean mass transfers. *J. Phys. Oceanogr.*, 31, 1623-1642..
- Dencausse, G., M. Arhan, S. Speich, 2010 : Spatio-temporal characteristics of the Agulhas Current Retroflexion. *Dees Sea Res*. In press.
- Dencausse, G., M. Arhan, S. Speich, 2010: Routes of Agulhas rings in the southeastern Cape Basin. *Deep Sea Res*. In press.
- Dencausse, G., M. Arhan, S. Speich, 2010 : Is there a continuous Subtropical Front south of Africa ? *J. Geophys. Res.*, accepted.

- Dong S., Gille S.T., Sprintall J., 2007: An assessment of the Southern Ocean mixed layer heat budget. *J Clim*, 20, 4425-4442.
- Duplessy, J. C. & Shackleton, N. J., 1985: Response of the deep-water circulation to the Earth's climatic change 135,000-107,000 years ago. *Nature* 316, 500-507.
- Faure, V., M. Arhan, S. Speich, and S. Gladyshev, 2011 : Heat budget of the surface mixed layer south of Africa. *Ocean Dyn.*, doi: 10.1007/s10236-011-0444-1.
- Garzoli S. L., Alberto Piola, Sabrina Speich, Molly Baringer, Gustavo Goni, Kathy Donohue, Chris Meinen, Ricardo Matano, 2007 : A monitoring system for heat and mass transports in the South Atlantic as a component of the Meridional Overturning Circulation. South Atlantic Meridional Overturning Circulation Workshop Report : http://www.aoml.noaa.gov/phod/SAMOC/SAMOC_report_January_08.pdf
- Gladyshev, S., M. Arhan, A. Sokov, S. Speich, 2008. A hydrographic section from South Africa to the southern limit of the Antarctic Circumpolar Current at the Greenwich meridian. *Deep Sea Res.*, 55, 1284-1303.
- Legeais, J.-F., S. Speich, M. Arhan, I. Ansorge, E. Fahrbach, S. Garzoli, et A. Klepikov, 2005 : The baroclinic transport of the Antarctic Circumpolar Current south of Africa. *Geophys. Res. Lett.*. doi :10.1029/2005GL023271.
- Lumpkin, R., and K. Speer, 2007: Global Ocean meridional overturning. *Journal of Physical Oceanography*, 37(10):2550-2562.
- McCartney M.S., 1977: Subantarctic mode water. In: Angel M. (ed), *A voyage of discovery*, Pergamon, New York, pp103-109.
- Ollitrault, M., and J.P. Rannou, 2010: ANDRO: An Argo-based deep displacement Atlas, *Joint Coriolis-Mercator Ocean Quarterly Newsletter*.
- Peeters, F. J. C. et al., 2004: Vigorous exchange between Indian and Atlantic ocean at the end of the past five glacial periods. *Nature* 430, 661-665.
- Rickaby, R. & Bard, E., 2009: Migration of the subtropical front as a modulator of glacial climate. *Nature* 460, 380-383.
- Rusciano, E., S. Speich, M. Arhan, M. Ollitrault, 2012: Observations of the interocean exchanges and spreading of the antarctic intermediate water south of africa. *J. Geophys. Res.*, To be submitted.
- Sallée J.-B., Speer K., Morrow R., Lumpkin R., 2008: An estimate of Lagrangian eddy statistics and diffusion in the mixed layer of the Southern Ocean. *J Mar Res*, 66, 441-463.
- Sallée J.-B., Wienders N., Speer K., Morrow R., 2006: Formation of subantarctic mode water in the southeastern Indian Ocean. *Ocean Dyn*, 56, 525-542.
- Sloyan, B. M. & Rintoul, S. R., 2000: Estimates of area-averaged diapycnal fluxes from basin-scale budgets. *J. Phys. Oceanogr.* 30, 2320-2341.
- Speich, S., J. Lutjeharms, P. Penven, B. Blanke, 2006 : The Indo-Atlantic exchange : dynamics of a regime transition from a western boundary current to an eastern boundary system. *Geophys. Res. Lett.*, VOL. 33, L23611, doi:10.1029/2006GL027157.
- Speich, S., B. Blanke, and W. Cai, 2007: Atlantic Meridional Overturning and the Southern Hemisphere Supergyre. *Geophys. Res. Lett.*, VOL. 34, L23614, doi:10.1029/2007GL031583.
- Speich, S., M. Arhan, 2007. ARGO floats sample vertically homogenized water in Agulhas Rings, *Coriolis Newsletter*, 4, 15-16.
- Speich, S., S. Garzoli, A. Piola and the SAMOC community, 2010: A monitoring system for the South Atlantic as a component of the MOC. In *Proceedings of OceanObs'09: Sustained Ocean Observations and Information for Society (Annex)*, Venice, Italy, 21-25 September 2009, Hall, J., Harrison, D.E. & Stammer, D., Eds., ESA Publication WPP-306.
- Stramma, L. & England, M., 1999: On the water mass and mean circulation of the South Atlantic Ocean. *J. Geophys. Res.* 104, 863-883 .
- Sun, C., and D. R. Watts 2001: A circumpolar gravest empirical mode for the Southern Ocean hydrography, *J. Geophys. Res.*, 106, 2833– 2855.
- Sun, C., and D. R. Watts, 2002: Heat flux carried by the Antarctic Circumpolar mean flow, *J. Geophys. Res.*, 107(C9), 3119, doi:10.1029/2001JC001187.
- Swart, S., S. Speich, I. Ansorge, G. J. Goni, S. Gladyshev, J. R. Lutjeharms, 2008. Transport and variability of the Antarctic Circumpolar Current south of Africa *J. Geophys. Res.*, 113, C09014, doi:10.1029/2007JC004223
- Swart, S., S. Speich, I. Ansorge, J. Lutjeharms, 2010: A satellite altimetry based Gravest Empirical Mode South of Africa. Part I: Development and Validation. *J. Geophys. Res.*, 115, C03002, doi:10.1029/2009JC005299.
- Swart, S., S. Speich, 2010: A satellite altimetry based Gravest Empirical Mode South of Africa. Part II: 1992-2008 Heat, Salt and Mass Transport variability and changes. *J. Geophys. Res.*, 115, C03003, doi:10.1029/2009JC005300.
- von Schuckmann, K., C. Cabanes, J.-B. Sallée, P. Y. Le Traon, F. Gaillard, S. Speich, M. Hamon, 2012: The role of Argo steric sea level within the global sea level budget. *J. Clim.*, to be submitted.
- Watts, R. D., C. Sun, and S. R. Rintoul, 2001, A two-dimensional gravest empirical mode determined from hydrographic observations in the Subantarctic Front, *J. Phys. Oceanogr.*, 31, 2186–2209.
- Weijer, W., De Ruijter, W. P. M., Sterl, A. & Drijfhout, S. S., 2002, Response of the Atlantic overturning circulation to South Atlantic sources of buoyancy. *Global and Planetary Change* 34, 293-311.

USE OF ALTIMETRIC AND WIND DATA TO DETECT THE ANOMALOUS LOSS OF SVP-TYPE DRIFTER'S DROGUE

By M-H. Rio⁽¹⁾

⁽¹⁾CLS, Toulouse, France

Introduction

In the framework of the SVP (Surface Velocity Program) and GDP (Global Drifter Program) programs, a large number of drifting buoys has been deployed in the ocean since the early 1980s with the objective to measure the ocean currents at a nominal depth of 15m. These drifters have been specifically designed to reduce the wind slippage to less than 0.1% in 10 m/s wind speed (Niiler et al, 1987, 1995). They consist of a surface float connected to a sub-surface 7 meter long holey sock drogue centered at 15m depth. In the original version (Sybrandy and Niiler, 1991), the drogue loss is detected by a change in the immersion behavior of the surface float through the use of a surface float submergence sensor. For more recent buoys, this was replaced by a tether strain gauge which monitors the tension between the buoy and the drogue. At AOML (Atlantic Oceanographic and Meteorological Laboratory), drifter trajectories are processed, quality controlled and 6-hourly velocities are computed that are distributed in delayed-time (Hansen and Poulain, 1996). Also, when appropriate, a drogue loss date is provided that allows discriminating between drogued and undrogued buoys.

The total current measured by a drifting buoy whose drogue is still on is the sum of various contributions including the geostrophic current, the Ekman current, and a number of other ageostrophic currents as inertial oscillations, tidal currents or Stoke's drift.

Thanks to the simultaneous measurement of the geostrophic surface currents by altimetry, the Ekman currents can be easily extracted from the drifter velocities. This was used several times

in the past to model the Ekman response \bar{u}_e of

the ocean currents to wind stress $\bar{\tau}$ by fitting a simple 2-parameters (β, θ) Ekman model like

$$\bar{u}_e = \beta \bar{\tau} e^{i\theta}$$

(Ralph and Niiler, 1999, Rio and Hernandez, 2003, Rio et al, 2011). Recently, Rio et al (2011) used the global dataset of 'drogued' drifting buoys distributed by AOML for the period 1993-2008 to update the Ekman model computed by Rio and Hernandez (2003). Surprisingly, the β and θ parameters were found to feature a decennial trend, with an increase of the β parameter by a factor of almost 3 over the entire period, and a decrease of the Ekman angle from 60° to 20°. (See Figure 6a,b of the Rio et al, 2011 paper and the black line in Figure 1 of the present paper). In Rio et al (2011), the authors are uncertain if the observed trend should be attributed to a real change in the ocean state or a potential change in the drifter design over time that would result in a change in the physical content of the velocities measured by the drifting buoy.

The recent paper by Grodsky et al, 2011 clearly pushed for the second explanation. A spurious trend in the drifter velocity dataset was detected, attributed to a problem of drogue loss detection that coincides with the introduction of a new drifter design in the mid 2000s (the 'mini SVP'). As a consequence, an increasing number of undrogued buoys pollutes the actual dataset of "drogued" drifting buoys distributed by AOML. In Grodsky et al (2011), the authors recommend using only the first three months of each drifter trajectory to enhance the probability of the drogue to be still on. We therefore have recomputed the β and θ parameters using the first three months of each drifter trajectory only (red curves on Figure 1). The decennial trend has almost entirely vanished, which means that the undetected undrogued drifters in the AOML "drogued" dataset are indeed responsible for the trend in the Ekman model parameters. However, both the β and the θ parameters still feature a spurious bound centered on 2004 so that we suspect that a number of drifters has lost the drogue in the first three months of their life. Furthermore, the truncation of the drifter trajectories to the first three months eliminates 90% of the drifter 6-hourly velocities measured during the 1993-2010 time period (Table 1).

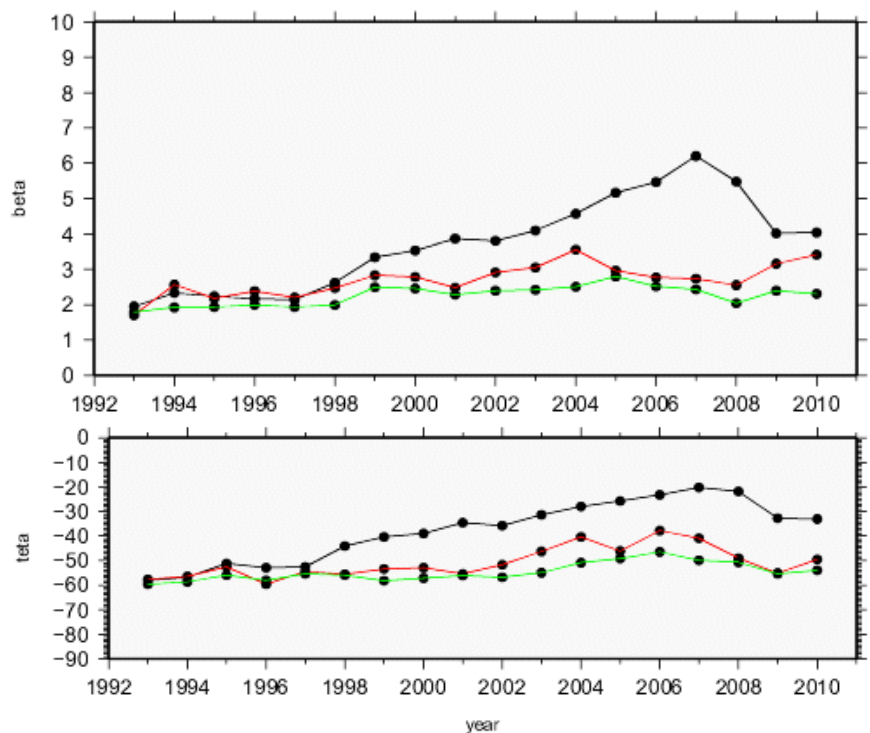


Figure 1 : Parameters β (top) and θ (bottom) of the Ekman model estimated yearly by least square fit. Black line: the AOML 'drogued' drifting buoy dataset has been used. Red line: Only the first three months of the 'drogued' AOML dataset has been used. Green line: Using only the buoy velocity flagged as 'drogued' by our methodology.

Nb velocity measurements						
All trajectories	Trajectories >200 days	Trajectories >200 days Excluding the first and the last 50 days	Flag AOML=1		Flag AOML=0	
			4,441,197		8,117,287	
			Flag _α =1	Flag _α =0	Flag _α =1	Flag _α =0
18,065,924	15,009,040	12,558,484	4,073,332 (92%)	367,865 (8%)	4,470,821 (55%)	3,646,466 (45%)

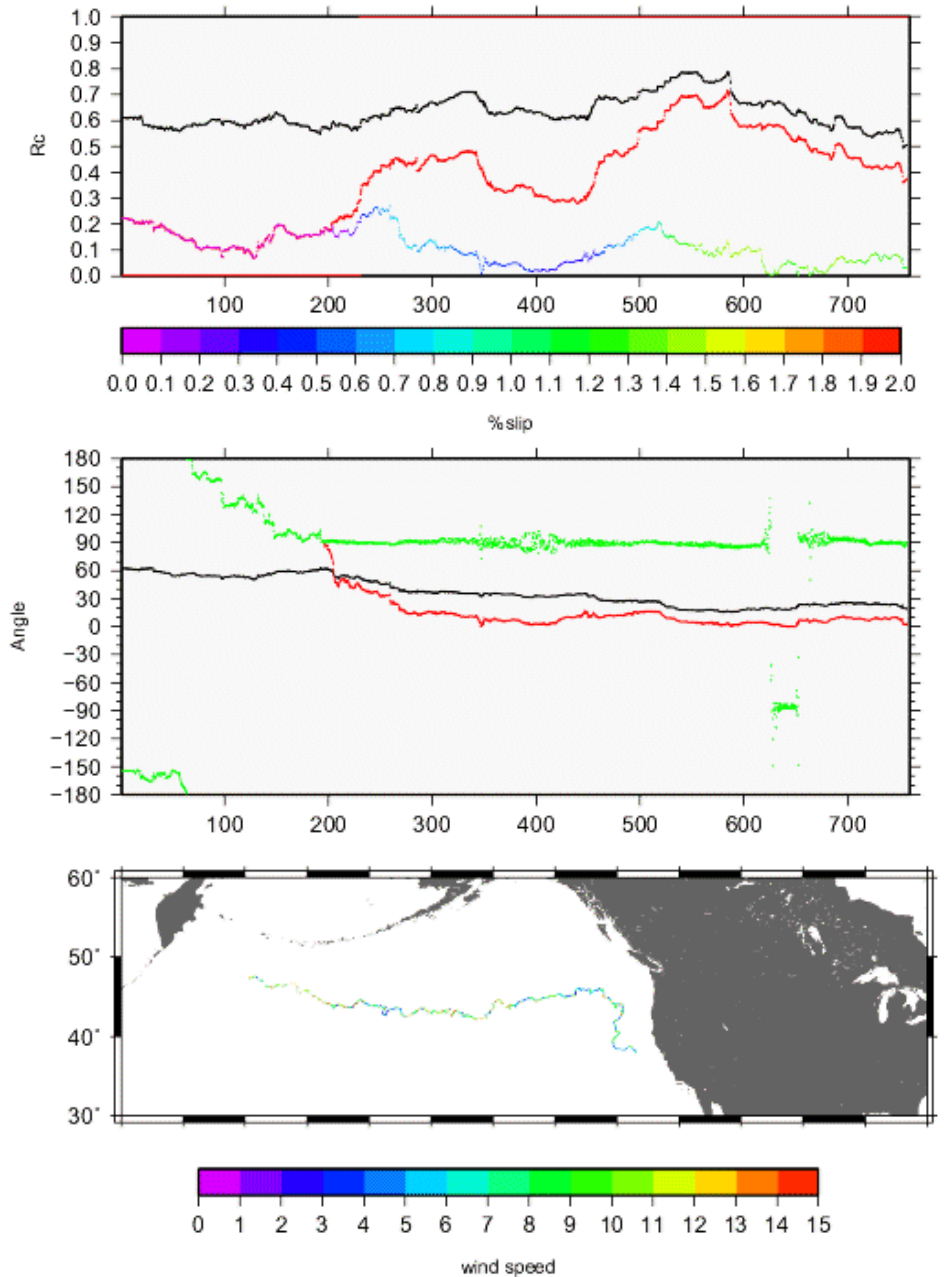
Table 1 : Number of velocity measurements contained in the different datasets used in this study. Flag AOML=0 (resp. 1) for “drogued” (resp. “undrogued”) drifter velocities. Flag_α refers to the flag defined if the text: It is 1 when α is greater than 0.3%, indicating a probable drogue loss.

As a consequence, a rigorous cleaning of the dataset is needed, which motivated the present study. In the following we present a simple approach based on the combined use of drifting buoys, wind and altimeter measurements that allows detecting the drifters’ drogue loss.

Detecting the drifter drogue loss: Method

The main idea of the method is to remove from each single drifter velocity the geostrophic and Ekman currents and see how well the residual velocity correlates to local wind. Residual velocities from buoys with the drogue attached should be uncorrelated to the wind while residual velocities from undrogued buoys (for which wind slippage is not negligible anymore) are expected to show a significant correlation to the wind.

Figure 2: Correlation coefficient (top) and angle (middle) between the wind velocity and the residual drifter velocities as a function of drift days. Black line: Residual velocities=Drifter velocities – geostrophic velocities. Red line: Residual velocities=Drifter velocities – geostrophic velocities–Ekman velocities. Green line in the middle plot and colored line in the top plot: Residual velocities=Drifter velocities–geostrophic velocities–Ekman velocities – αWind where α is computed to minimize the correlation coefficient. The color scales in the top plot gives the value of α. The flag indicating drogue presence is set to 1 when α exceeds 0.3 (red line in top plot). Bottom plot: Drifter trajectory. Colors indicate the wind speed (m/s).



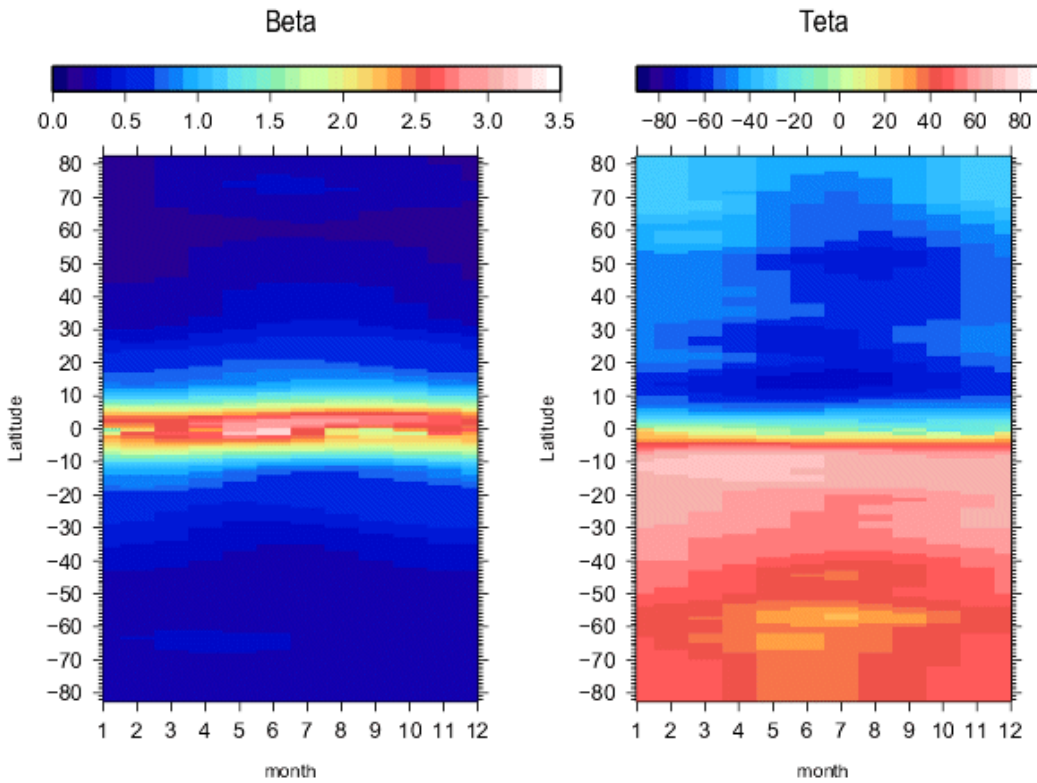


Figure 3 : Parameters β (left) and ϑ (right) of the Ekman model estimated by latitude and by month using only the first three months of the trajectories from the 'drogued' AOML dataset.

Data

In addition to the drifting buoy dataset described above, two types of data have been used for this study. First, altimetric multimission, delayed mode, $1/3^\circ$ resolution maps of absolute geostrophic surface currents computed at CLS and distributed by AVISO have been used for the period 1993-2010.

Also, we have used 3-hourly, global, 80 km resolution wind stress maps from the ERA INTERIM reanalysis (Simmons et al. 2006). Wind values

$$W = \sqrt{\frac{\tau}{\rho_a C_D}}$$

W have been computed from the wind stress using a simple bulk formula, 10^{-3} is a non dimensional drag coefficient.

where $\rho_a=1.3 \text{ kg}\cdot\text{m}^{-3}$ is the air density and $C_D=1.4$

Results

First, the altimetric maps of absolute geostrophic currents were interpolated along the drifter trajectories and subtracted from the drifter velocities. Then a 3-days low pass filter was applied to remove the inertial oscillations, the tidal currents and the other high frequency ageostrophic currents. The obtained residual velocity is an estimate of the Ekman response to wind stress. The wind values were also interpolated along the drifter trajectory and the vectorial correlation between the drifter residual velocity and the wind speed was computed along each single drifter trajectory using a 100 days moving window. Consequently, only drifter trajectories longer than 200 days were used. Furthermore, by construction, no correlation could be computed for the first and the last 50 days. The black line in Figure 2 shows the vectorial correlation (top) and the correlation angle (middle) obtained for a buoy that has drifted during more than 2 years in the North East Pacific ocean (bottom plot). During the first 250 days, the correlation coefficient is around 0.6 and the correlation angle is around 60° , in good agreement with the Ekman response of the surface currents to the wind.

Then a new "residual" drifter velocity (hereafter $\vec{u}_{\text{residual}}$) was computed along each single trajectory removing both the geostrophic velocity and the Ekman velocity from the drifter velocity and further applying a 3-days low pass filter. The Ekman model used at this stage of the study was computed by latitude and by month using only the first three months of the drifting buoy trajectories. Obtained values are displayed on Figure 3. We observe a decrease of both the angle and the amplitude response of surface currents to wind stress in winter and at high latitudes in good consistency with a decrease in stratification.

Vectorial correlations were then computed between $\vec{u}_{\text{residual}}$ and the wind speed (red lines in Figure 2). During the first 250 days correlation coefficient values lower than 0.3 are obtained as well as correlation angles switching from plus to minus 180° . After 250 days, the correlation coefficient increases and the correlation angle gets close to 0° , suggesting that the buoy is most probably drifting with the wind. For this particular trajectory, we are therefore confident that the buoy has lost its drogue after 250 days drift.

Finally, the colored line on Figure 2 gives the value of a coefficient α allowing to minimize the correlation between the wind and a third resid-

$$\vec{u}_{\text{residual}\alpha} = \vec{u}_{\text{residual}} - \alpha \vec{W}$$

ual drifter velocity defined as $\vec{u}_{\text{residual}\alpha}$. For drogued buoys, this coefficient was estimated to be less than 0.001 in 10 m/s wind condition by (Niiler et al, 1987). This is the case indeed for the first 200 days of the trajectory in Figure 2. Then α increases and remains greater than 0.3%.

Figure 2 is an example given for a specific trajectory, but the whole dataset was processed and the α parameter was found to be quite a good indicator of the drogue presence. Consequently we set up an automatic detection of the drifter drogue loss by defining a threshold value for α equal to 0.3% above which the drifter was considered to have most probably lost its drogue.

Figure 4 shows the average into 20° by 20° boxes of the α parameters when greater than 0.3%. Highest mean values (1.5%) are obtained in the Antarctic Circumpolar Current

Method robustness

In order to test the robustness of this simple detection procedure we applied it on the whole AOML drifter dataset, including the known undrogued drifters. Again, only trajectories longer than 200 days were kept and the methodology used prevents from determining the drogue presence for the first and last 50 days. This restriction removes 16% of the total velocity dataset (table 1).

Among the remaining 12,558,484 velocity measurements (drogued and undrogued drifter velocities), 35 % are flagged as undrogued by AOML (table 1). This absence of drogue is detected by our method in 92% of the cases, which makes us confident in the capability of our simple approach to detect the drifter drogue loss. Regarding the remaining 65% of data where the drifter is flagged as 'drogued' by AOML, our methodology detects 55% of undrogued data. This means that from the original dataset of 12,558,484 velocity measurements, only 30% are considered as measured by a drogued drifter by our methodology (instead of 65% for AOML).

Mean wind slippage of undrogued buoys

In addition to providing a good indicator of the drifter drogue presence, the methodology developed in this study allows estimating a correction term to the velocity measured by an undrogued drifter. In effect, for each velocity measurement, the computed α coefficient times the wind is the drifter velocity component due to the direct wind effect on the buoy. It may be subtracted from the measured velocity to compute a corrected velocity value in order not to discard the velocity measurements from drifting buoys having lost their drogue (55% of the AOML 'drogued' dataset).

Figure 5 shows the mean corrected term computed in 20° by 20° boxes over the global ocean from the undrogued buoy velocities. It exceeds 10 cm/s in the Antarctic Circumpolar area and 2-4 cm/s almost everywhere else. If only drifters with the drogue on are considered, this mean corrective term is found to be less than 1 cm/s everywhere (not shown).

Conclusion

Recent and repeated failures in the SVP-type drifter drogue loss detection system (based on tether strain gauge or submergence tests) have led to an increasing number of undrogued drifters into the "drogued" drifters dataset distributed by AOML (Grotsky et al, 2011). This problem is found to fully explain the anomalous decennial variability of the Ekman response to wind stress detected by (Rio et al, 2011). In this study a simple methodology has been developed that allows detecting the drifter drogue loss and providing an estimate of the wind slippage to be used as a velocity correction. Our approach correctly detects 92% of the AOML known undrogued drifter velocities and removes 55% of the velocity measurements from the AOML "drogued" dataset. When averaged over the full 1993-2010 period and in 20° by 20° boxes, the wind slippage affecting these undrogued buoys is found to exceed 10 cm/s in the Antarctic Circumpolar Current.

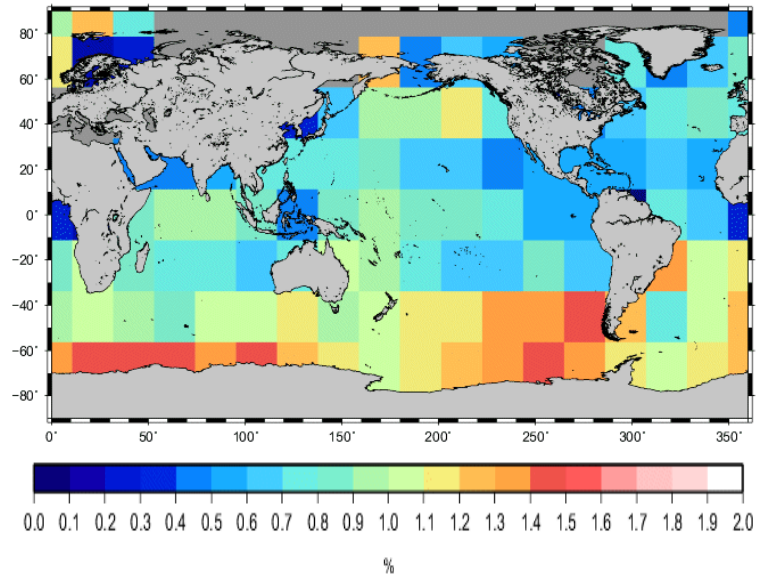


Figure 4 : Average in 20° by 20° boxes of the α coefficient obtained for the drifters flagged as having lost their drogue by our methodology.

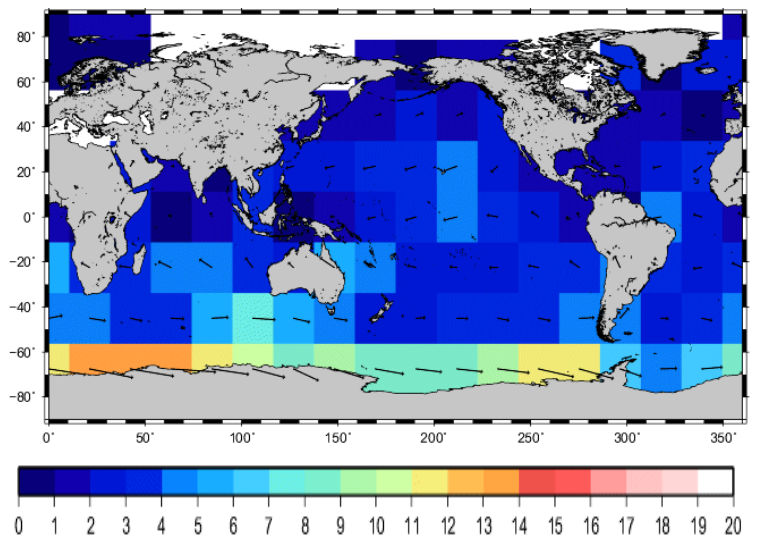


Figure 5 : Mean wind slippage (cm/s), computed in 20° by 20° boxes of the drifters flagged as having lost their drogue by our methodology.

The methodology presented here suffers some limitations. First it is limited to drifter's trajectory longer than 200 days. Moreover, the first and the last 50 days cannot be processed, since the correlation between the wind and the residual velocities runs along 100 days segments of the drifter trajectory. Finally, the present work was done on delayed-time data and further developments would be needed to detect the drogue loss in real time.

References

- Grodsky, S. A., R. Lumpkin, and J. A. Carton (2011), Spurious trends in global surface drifter currents, *Geophys. Res. Lett.*, **38**, L10606, doi:10.1029/2011GL047393
- Hansen, D. V., and P.-M. Poulain, Quality control and interpolation of WOCE/TOGA drifter data, *J. Atmos. Oceanic Technol.*, **13**, 900–909, 1996.
- Niiler, P. P., R. Davis, and H. White (1987), Water-following characteristics of a mixed-layer drifter, *Deep Sea Res., Part A*, **34**, 1867–1881, doi:10.1016/0198-0149(87)90060-4.
- Niiler, P. P., A. S. Sybrandy, K. Bi, P. M. Poulain, and D. Bitterman (1995), Measurements of the water-following capability of holey-sock and TRISTAR drifters, *Deep Sea Res., Part I*, **42**, 1951–1964, doi:10.1016/0967-0637(95)00076-3.
- Ralph, Elise A., Pearn P. Niiler, P. P., 1999: Wind-Driven Currents in the Tropical Pacific, *Journal of Physical Oceanography*, **29**, 2121-2129
- Rio, M.-H. and F. Hernandez, 2003: High-frequency response of wind-driven currents measured by drifting buoys and altimetry over the world ocean. *Journal of Geophysical Research* **108**(C8): 3283-3301
- Rio, M. H., S. Guinehut, and G. Larnicol, 2011: New CNES-CLS09 global mean dynamic topography computed from the combination of GRACE data, altimetry, and in situ measurements, *J. Geophys. Res.*, **116**, C07018, doi:10.1029/2010JC006505.
- Simmons A., Uppala, S., Dee, D., Kobayashi, S., 2007. ERA-Interim: New ECMWF reanalysis products from 1989 onwards. *ECMWF Newsletter* **110**, 25–35.
- Sybrandy, A L, Pearn P Niiler, 1991. WOCE/ TOGA Lagrangian drifter construction manual. WOCE Report No 63; SIO Report No 91/6. Scripps Institution of Oceanography, La Jolla.

SURFACE SALINITY DRIFTERS FOR SMOS VALIDATION

By **S. Morisset⁽¹⁾, G. Reverdin⁽¹⁾, J. Boutin⁽¹⁾, N. Martin⁽¹⁾, X. Yin⁽¹⁾, F. Gaillard⁽²⁾, P. Blouch⁽³⁾, J. Rolland⁽³⁾, J. Font⁽⁴⁾, J. Salvador⁽⁴⁾**

⁽¹⁾LOCEAN/IPSL, UMR CNRS/UPMC/IRD/MNHN, Paris, France

⁽²⁾LPO, IFREMER, Plouzané France

⁽³⁾CMM, Météo-France, Brest, France

⁽⁴⁾ICM/CSIC, Barcelone, Spain

Introduction

The ESA/SMOS (European Space Agency/Soil Moisture and Ocean Salinity) satellite mission provides new measurements of Sea Surface Salinity (SSS) using L-band radiometry. After correcting SMOS brightness temperatures from systematic biases, SMOS sea surface salinity (SSS) reproduces quite well large scale expected SSS variations [Font et al., 2012].

At L-band frequency, the skin depth is 1 centimetre while most in situ SSS measurements are taken at a few meters depth. A preliminary study based on ARGO vertical profiles [Henocq et al., 2010] indicated that vertical salinity differences between 1m and 10m depth higher than 0.1 psu are observed in the 3 oceans, mainly between 0° and 15°N, coinciding with the average position of the Inter Tropical Convergence Zones characterized by high precipitation rates.

In order to better document the variability of salinity near the sea surface, which is currently not often measured by other in situ observations (current Argo uppermost data is between 5 and 10m depth, whereas TAO-type measurements are near 1 or 2m depth), surface drifters have been equipped with Conductivity-Temperature (C-T) cells near a depth of 50 cm, which proved reliable for mid-latitude deployments [Reverdin et al., 2007]. Since then, two manufacturers of SVP (Surface Velocity Program) drifters, Metocean and the Pacific Gyre have instrumented SVP drifters with sensors measuring conductivity at 30-50cm depth. In addition, new light floats named SURPLAS have been built at LOCEAN laboratory to measure conductivity at 15cm depth for a duration of a few weeks to a few months. SURPLAS floats have been tied to SVP drifters allowing the study of the SSS and SST (Sea Surface Temperature) stratification between 15cm and 50cm depth. In addition, ICM/CSIC has built slightly larger drifters with C-T cells also near 50 cm depth, but without an anti-fouling protection of the cell. The sampling characteristics of the different drifters are slightly different. The SURPLAS drifter provides a value (average over 8") every 15 minutes of T (Temperature) and S (Salinity); the Pacificgyre SVP-BS drifter, a value every 30 minutes (average over 5 minutes), the Metocean SVP-BS drifter, a value every hour (average of 7 values over 10 minutes), and the ICM/CSIC provide values at the time of Argos transmissions (not averaged). Most of the drifters and floats transmit through Argos, although Metocean drifters since 2009 mostly transmit data (and a 3-hourly gps position) through iridium communication.

Since 2007, we deployed 37 Metocean SVP-BS drifters, 29 Pacificgyre drifters, 21 ICM/CSIC drifters and 17 surplus floats. In 2010 and 2011, simultaneous to the first two years of SMOS measurements, 68 SVP drifters (49 Metocean and PacificGyre and 19 ICM drifters) and 13 SURPLAS floats have been deployed by the French and Spanish teams involved in the SMOS Cal/Val projects mostly in the North Atlantic, in the Bay of Biscay, in the equatorial and subtropical South Atlantic and in the western tropical and equatorial Pacific Ocean. Altogether in 2010-2011, they recorded measurements during 13500 days (Metocean+PacificGyre 8821, Surplax 472, ICM 4266).

In this paper, we will first comment on the data return of these drifters, on our efforts to quality control and correct the data. Then, we will summarize results on tropical SSS freshening events linked to rain events as recorded at various depths by autonomous drifters and as deduced from the SMOS radiometer measurements.

Data return of the drifters – validation/correction of the data

The SVP and ICM drifters had an average life time in the water that was most commonly shorter than 1 year, mostly because of recovery by fishermen (7 in the Bay of Biscay and near Atlantic region, 6 near South America/Caribbean and one each off Ivory Coast and off Queensland), because of landing most commonly after a drogue loss. In some instances (in the Bay of Biscay, Queensland coast or off Ireland), the recovery was done on purpose and the drifter redeployed soon after (but we consider this as two separate drifters in our accounting). For some of the drifters (6 Metocean with mean lifetime of 14 month, and one Pacificgyre with lifetime of 21 months), the death occurred through normal battery loss.

Data interruption occurred quickly through switch problems for 4 Pacificgyre, through electronic problems for 2 Pacificgyre, and through unknown reasons for 4 Pacificgyre. For two Metocean drifters, there was C-T data loss after a while, and for 9 Metocean drifters, end of life probably happened through electronics or leak after a short while (5 presented a visible fast fall of the battery tension beforehand).

Drogue loss seems to have happened often within less than 6 months at sea, although we did not investigate carefully the issue of drogue loss of these drifters, and it is possible (Gordisky and Lumpkin, 2011) that residual errors in drogue loss detection might be present in this data

set (although, we use a larger drifter model than the ones that are suspicious according to Gordsky and Lumpkin (2011)).

In another paper, we have commented that there are errors in the regular hull temperature sensor of the drifters (Reverdin et al., 2009). We assume that the biases on the T sensor of the C-T cell is very small (could be of the order of 0.01°C according to Seabird after 1 year in the water); thus we can use this T to validate the hull temperature sensor (referred here as SST). We find rather large (0.5°C or larger) anomalies in 2010 on both Metocean and Pacificyre drifters, but which have been explained by conditions in which this temperature was controlled. The problem has disappeared with later deliveries in 2011, but there are still issues with this measurement on 2011 Pacificyre drifters (data become very noisy and unusable after a few to six months, probably as the result of leak or electronic issues).

Five Metocean drifters deployed in the Amazon plume or off French Guyana presented large drops of salinity that are surely attributable to algae or other floating objects that got stuck in the cell. One of these drifters was recovered, rinsed and redeployed with no indication of sensor fouling. For most of the ICM drifters deployed in the subtropical gyres, large drops in salinity occurred within a few months that could be due either to objects stuck in the cells or fouling, as these drifter sensors were not protected by anti-fouling. In these cases, we don't feel that we can recover a usable salinity data, and prefer to remove the estimated S from the final files.

This leaves an average 5 month of usable salinity data by Pacificyre drifter and 6 months by Metocean drifter. On these data, we apply the following checks to eliminate dubious portions of the records.

First, we check temperature measurements. Some isolated measurements can be incorrect in the first hours after deployment (hull temperature) or due to bias transmission (example 0.01% of data for long-lived PacificGyre 92546). Associated salinities are removed.

Removal of salinity for periods with unusual high noise level (probably some moving objects or electronic problems) as well as removal of isolated salinity spikes with a filter is performed. The filter identifies isolated values deviating from the median of salinity measured between 6 hours before and 6 hours later and larger than twice the standard deviation for the same period. We then check whether there is regular increase of salinity during the two following points after the isolated spike, in which case we retain the isolated value (which could result from front or rainfall passing) (the removed isolated data represent 0.4% for PacificGyre drifter 92546).

We then remove S values during mid-day warming periods, as we had shown (for 2005 drifters) that the mismatch between C and T sensors can be the origin of large mid-day errors (Reverdin et al., 2005). For that, we check whether daily warming is larger than 0.8°C, and remove mid-day data, when they present variability (for example, this represents 3% of data for PG drifter 92546; note that this was difficult to apply on ICM drifters that often transmit data only during the 6 hours each day between 0 and 6 GMT).

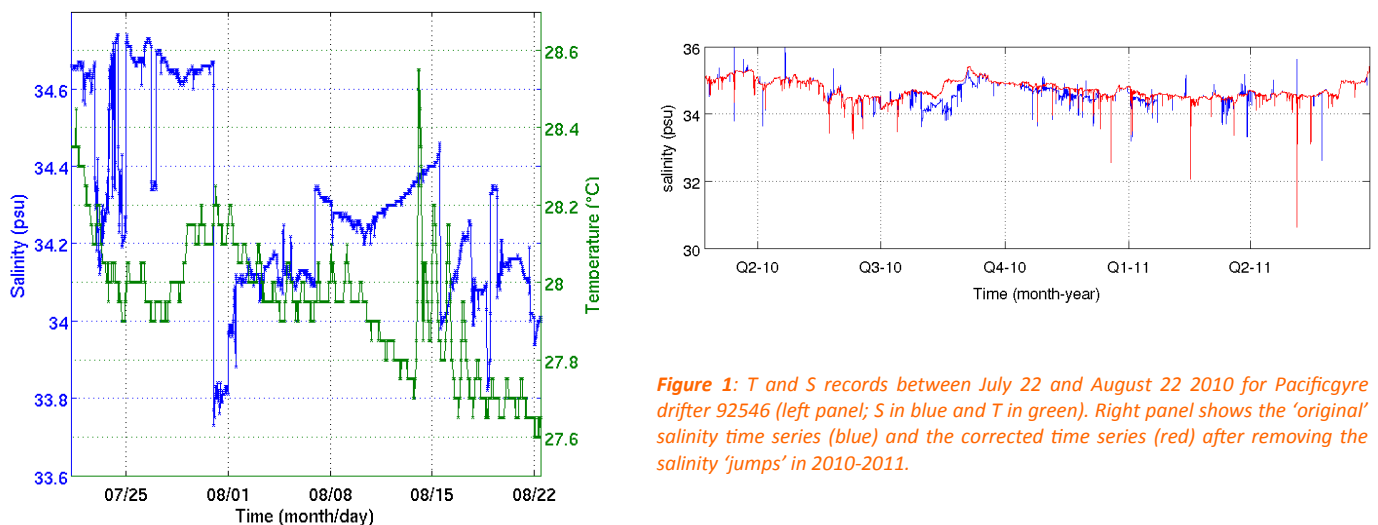


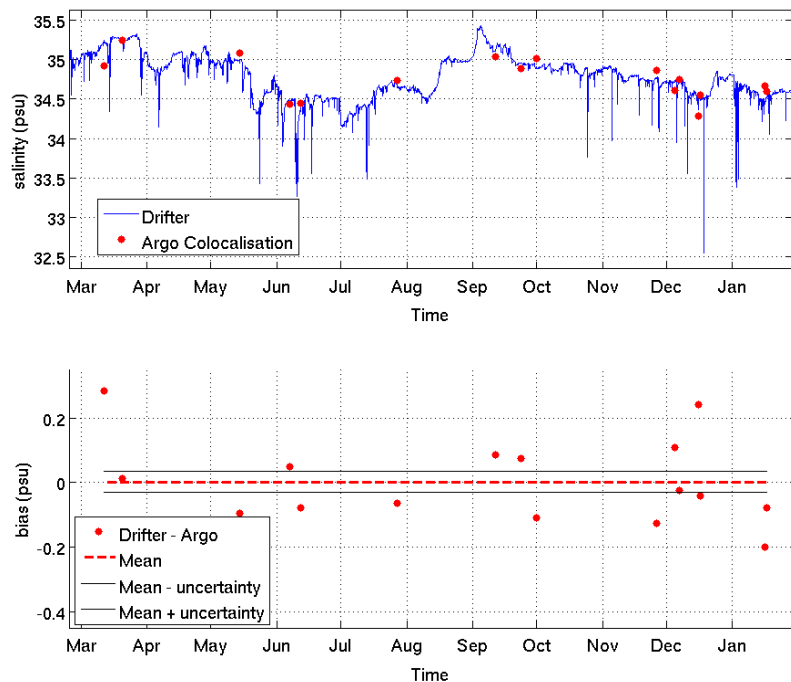
Figure 1: T and S records between July 22 and August 22 2010 for PacificGyre drifter 92546 (left panel; S in blue and T in green). Right panel shows the 'original' salinity time series (blue) and the corrected time series (red) after removing the salinity 'jumps' in 2010-2011.

In some data records, we observe sudden changes of S, with no corresponding change of T (changes less than 0.05°C). They are first a decrease of salinity, but can be also afterwards with a salinity increase. In a few cases, when we had a surplus float attached to the SVP drifter, we can clearly confirm that these jumps are not real S-jumps, probably associated with objects stuck in the cell. We also found at least one case with a jump of S, where the associated change in T was less than 0.05°C. This is an issue, as before the Iridium Metocean models and the 2011 Pacificyre models, the resolution in temperature was on the order of 0.05°C, and such a 'real' S-jump would be interpreted as erroneous. Nonetheless, we consider most of these S-jumps with no T-jump larger than 0.05°C as highly dubious, and we try to correct the data after the jump by adjusting their value to the one just before (clearly, this leaves an uncertainty in each adjustment of at least 0.01 ps). We present an example of a time series which presents such jumps, as well as the value at the shallowest level of ARGO float profiles.

This kind of sudden jumps happened in different instances for this drifter, and the final record is presented below. In this case, the upper values of nearby Argo profilers fit well with the corrected time series, and we have little doubts that the jumps were really related to objects getting stuck in the cell.

The drifter records were systematically compared with upper values (between 5 and 10m depths) of near-by ARGO profiles. We retain those values only if the ARGO temperature is close to the one measured by the drifter (at night). Often there are enough Argo profiles to be able to statistically identify (by grouping the comparisons over a long-enough period) a possible drift due to fouling of the sensor. We sometimes

Figure 2: upper panel, the corrected S records of the 92546 salinity drifter with the colocated ARGO profiles values (red) from February 2010 to January 2011. The lower panel show the differences (red dots) with the suggested bias (dashed line with the 1-sigma uncertainty range).



also have samples collected at recovery or when a ship passed near-by that provide another estimate of the drift. Often, these comparisons suggest that the bias is small in the first 6-months of the drifter life (except for the ICM drifters). When we have more than one such comparison (usually only for mid-latitude or high latitude drifters), we assume that the drift varies linearly in time. Clearly, this degrades the accuracy of the drifter data (typically, for the ones we have compared, only after a year or more).

The longer time series in the tropics can be analysed in relation to rainfall events, but also to possible daily cycles. So far, and except close to Africa, the salinity daily cycles identified have been very small (on the order of 0.01 psu or less), which is consistent with earlier analyses of the TAO/TRITON mooring data).

Freshening events observed by the drifters

[Reverdin et al., 2012] have analyzed the drifter measurements in the tropical oceans in 2007-2010 and have isolated individual freshening events by seeking salinity drops larger than 0.1 psu that are nearly compensated (80) within one day. These events which average 0.56 psu at 45 cm are often related (at least 50% of the cases) with local rainfall. When two measurement levels are available (with a surplus float attached to a SVP drifter), the initial salinity signal is larger by more than 20% at the shallow depth (15 cm) compared with the deeper measurement level (near 50 cm) (Figure 2).

These salinity drops are often associated with a temperature drop which also presents a gradient between the two levels. This temperature drop gradient is to some extent related to the cooler temperature of the drops, but also to the surface stratification created by the rain, such that the heat loss related to the latent (and sensible) heat losses is trapped very close to the surface.

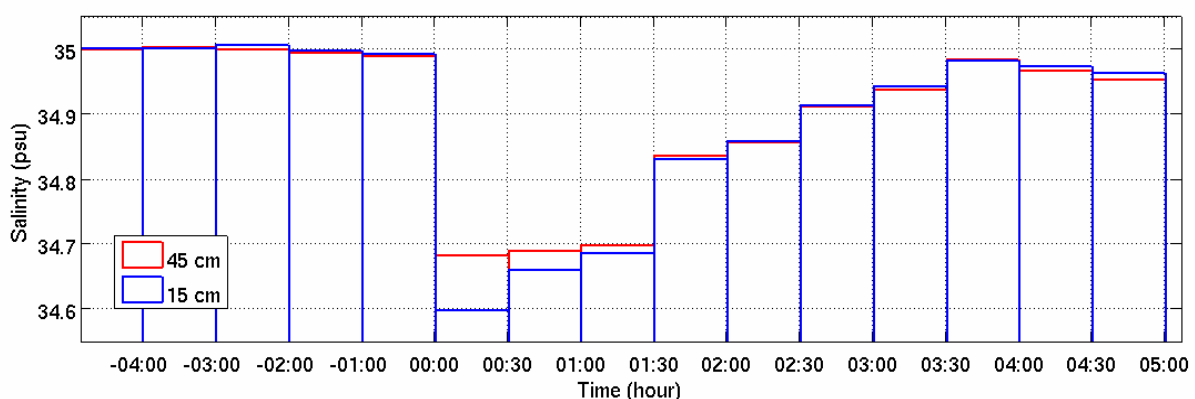


Figure 3: Average composite cycle of salinity among 20 salinity drop events observed by both SVP-BS at 45 cm depth (red) and Surplus drifters at 15 cm depth (blue) (relative to a common time of beginning of event). Individual records are shifted to a common salinity value at the initial drop time.

Freshening events observed by SMOS

Comparisons between reprocessed SMOS SSS and ARGO SSS at 5m depth have been performed in the subtropical North Atlantic Ocean, in the region where the 2012-2013 “Salinity Processes in the Upper Ocean Regional Study” (SPURS) experiments dedicated to the calibration and validation of SMOS and Aquarius satellite measurements will take place. They indicate a standard deviation of the difference of 0.2psu once SMOS SSS are averaged over typical GODAE scales (10days-one month, 100kmx100km). On another hand, the same kind of comparison in the Intertropical Convergence Zone (ITCZ) of the Pacific Ocean indicates a standard deviation of the difference of 0.4psu and a mean difference 0.1psu lower in the ITCZ than in the SPURS region.

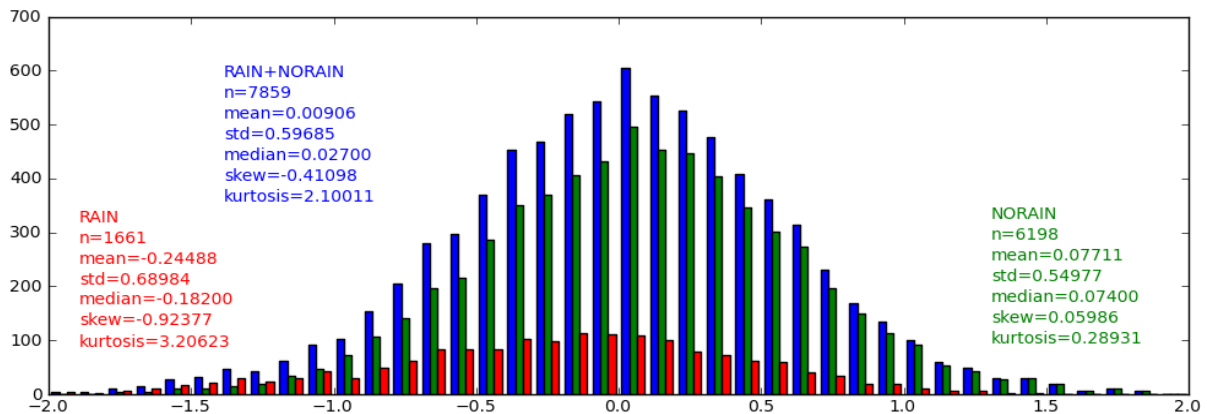


Figure 4: Statistical distribution of (SMOS SSS minus ARGO SSS) differences in the ITCZ of the Pacific Ocean (5°N-15°N-110°W-180°W) in July 2010. Blue distribution is obtained whatever the SSM/I rain rates (up to 10mm/hr) recorded within -80 mn before and +40 mn after SMOS measurement; green distribution corresponds to situations when no rain has been detected by SSM/I before SMOS measurement, red distribution corresponds to situations when SSM/I has detected non zero rain rates within 5 hours before SMOS measurement.

Collocations of (SMOS SSS minus ARGO SSS) differences with SSM/I rain rates recorded within -80 mn before and +40 mn after SMOS measurements show that the larger standard deviation and the negative difference in the ITCZ are mainly attributable to rain events.

In addition, we observe a significant correlation ($r=0.47$) between (SMOS SSS minus ARGO SSS) and SSM/I rain rates with a slope equal to 0.2psu/mm/hr.

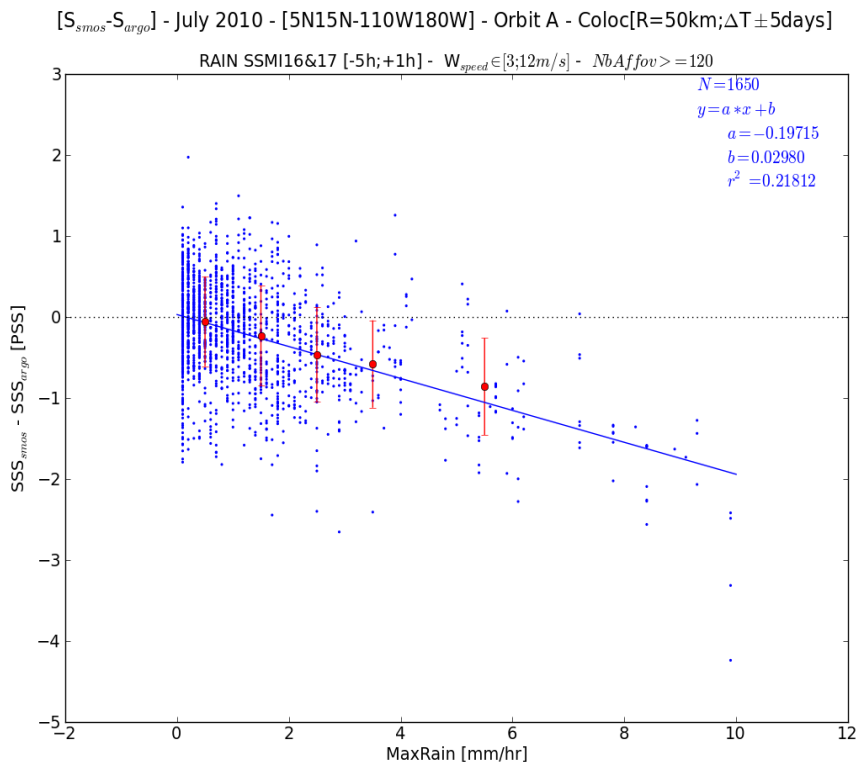


Figure 5: SMOS SSS minus ARGO SSS versus SSM/I rain rate observed within -80 mn before and +40 mn, after the SMOS SSS (July 2010; SMOS reprocessing version 5). Red points correspond to averages and standard deviations of SSS differences in 1mm/hr classes. The least square fit indicates a slope of -0.2psu/mm/hr.

Summary and perspectives

The surface drifters measuring sea surface salinity in the top 50cm of the sea surface provide a complementary source of data for validating L-band sea surface salinity. Previous comparisons with SMOS SSS indicate a precision of about .3psu in tropical regions, far from land. These comparisons will be re-evaluated with the 2011 SMOS reprocessing, in order to assess the improvement of the reprocessing especially close to land.

In addition, drifters identify significant rain salinity freshening in the tropical regions. The SMOS SSS reprocessing tested in July 2010 indicates a mean monthly freshening (-0.1 SSS bias averaged over the tropical Pacific between 5°N and 15°N) with respect to ARGO salinity at 5m depth. This salinity freshening is significantly correlated with rain events (identified on maximum SSM/I rain rate) occurring 5 hours before SMOS measurement ($R=0.47$) and is large: -0.2psu/mm/hr. Preparatory studies to SMOS [Schulz et al., 2002] and to Aquarius [Wentz, 2005] indicate that the atmospheric contribution of rain to L-band brightness temperature are smaller than at higher frequency, on the order of 0.2°K for a rain rate of 10mm/hr, which would correspond to a SSS bias of ~-0.4psu for a rain rate of 10mm/hr: this is an order of magnitude smaller than what we observe. In addition, according to [Schulz et al., 2002] and [Wentz, 2005], for non nadir measurements, the signature of rain atmospheric contribution is larger in horizontal polarisation than in vertical polarisation, contrary to what is expected from a contribution from sea surface salinity. Such a polarized signature should affect the SMOS retrieved wind speed, while salinity retrievals are only very slightly modified in rainy cases. In the next months, we will investigate further the angular signature of rainy events on SMOS brightness temperature in horizontal and vertical polarization (from 0° to 50° incidence angle) in order to better assess the precision of the sea surface salinity retrieved from SMOS measurements.

Salinity drifters will be deployed in 2012 and 2013 by various agencies, probably at the level of 100 drifters each year, in particular within the SPURS subtropical North Atlantic experiment, but also in the wet tropics. They will thus provide in those regions a significant amount of data complementing the other components of the upper ocean in situ observing system, and to help better understand near-surface stratification, when used together satellite retrievals from SMOS and AQUARIUS missions.

Acknowledgments

This effort is part of ESA for SMOS cal-val projects, and is supported nationally in France by CNES/TOSCA with the Gloscal project and in Spain at ICM/CSIC by the Spanish national R+D plan (project AYA2010-22062-C05). The deployments and recoveries of drifters were done from a large array of national research vessels and opportunity merchant or sailing vessels, to which we are highly indebted. The validated data can be retrieved under regions on <http://www.locean-ipsl.upmc.fr/smos/drifters>.

References

- Boutin et al., "Sea Surface Salinity from SMOS satellite and in situ observations: surface autonomous drifters in the tropical Atlantic Ocean", SMOS Science Workshop, Arles, Sept. 2011 (extended abstract).
- Cronin, M.F., and M.J. McPhaden (1999), Diurnal cycle of rainfall and surface salinity in the western Pacific warm pool, *Geophys. Res. Lett.*, 26, 3465-3468.
- Font, J., J. Boutin, N. Reul, P. Spurgeon, J. Ballabrera-Poy, A. Chuprin, C. Gabarro, J. Gouillon, S. Guimard, C. Hénocq et al., "SMOS first data analysis for sea surface salinity determination", *Int. J. of Rem. Sens.*, in press, 2011.
- Hénocq, C., J. Boutin, G. Reverdin, F. Petitcolin, S. Arnault, P. Lattes, "Vertical Variability of Near-Surface Salinity in the Tropics: Consequences for L-Band Radiometer Calibration and Validation". *J. of Atm. and Ocean. Technol.*, 27, 192-209, 2010.
- Reverdin, G., P. Blouch, J. Boutin, P. Niiler, J. Rolland, W. Scuba, A. Lourenço, A. Rios, 2007. Surface salinity measurements – COSMOS 2005 experiment in the Bay of Biscay. *J. Atmos. and Ocean. Tech.*, 24, 1643-1654.
- Reverdin, G., S. Morisset, J. Boutin, and N. Martin, Rain-induced variability of near sea-surface T and S from drifter data" [Paper #2011JC007549] *J. of Geophys. Res. – Oceans*, in Press, 2012.
- Schulz, J., Impact of rain on sea surface brightness temperature, in "Scientific requirements and impact of space observations of ocean salinity for modelling and climate studies", Nansen Environmental and Remote Sensing Center Technical Report no. 214, subtask 1200, pp 51-59, ESA contract 14273/00/NL/DC, 2002.[Available on the web at http://esamultimedia.esa.int/docs/Study_14273_FR.pdf]
- Wentz F. J., "The effect of clouds and Rain on Aquarius Salinity Retrieval", RSS Technical Memorandum 3031805, 2005.[Available on the web at http://www.ssmi.com/papers/aquarius/rain_effect_on_salinity.pdf]

A NEW INFORMATION AND DATA MINING TOOL FOR NORTH ATLANTIC ARGO DATA

By **G. Maze**⁽¹⁾

⁽¹⁾LPO, IFREMER, Plouzané France

The global Argo array is made of about 3,000 free-drifting floats measuring temperature and salinity (along with possibly other parameters such as oxygen) of the upper ocean. This continuous ocean monitoring in space and time produces a tremendous amount of data, made publicly available within hours. Argo data are available for download on ftp servers hosted by the two GDACs (Global Data Assembly Centers: USGODAE and Coriolis). As of February 2012, more than 900,000 NetCDF profile files were available on these servers. From the user perspective, especially new ones, engaging with such an amount of data may be impressive, and a laborious task.

Hence, as a complementary to other online services, a new information and data mining tool for Argo data in the North Atlantic have been designed to help users manipulating the data. This is a contribution to the North Atlantic Argo Regional Center (NA-ARC) and therefore only concerns Argo profiles located in North Atlantic Ocean North of 20°S, as well as in the Mediterranean and Arctic Seas.

This new tool aims at:

- Providing an interactive user interface for Argo data mining,
- Simplifying access to information about all, or a sub-set of, profiles,
- Centralizing as much as possible information provided by other services.

Specifically, the tool is made of a website and of a web service or web API (Application Programming Interface). The website provides the user interface to services provided by the web API. The latter is public in order to allow access to services programmatically. I will now present first the database used by the system, then the website and finally the web API.

The database

Every day at 0H00 GMT, the tool scans all NetCDF profile files on the Coriolis ftp server and selects those located in the NA-ARC region. Only profiles having a POSITION_QC flag of 1, 2, 5 or 8 are selected, meaning that the position in space and time of profiles is very likely correct. A database is then created with relevant information about these profiles, such as: spatio/temporal coordinates, Data Assembly Center name, WMO (World Meteorological Organization float unique ID) and cycle number, data mode, station parameters and profiles parameters QC flags (indicating the percentage of 'good' measurements for each of these parameters). The system complements this database with additional information from other sources:

- *Quality control* information retrieved from the ftp greylist file, the LPO/Argo quality control database and the CLS/Altimetry last test results. Floats or profiles reported by one of these sources are flagged as having a "ticket" in the database. More information will be incorporated in the future, such as the Objective Analysis Warning report.
- *Descriptive* information about measurements, primarily URL pointing to figures produced by Coriolis for each parameters and profiles.

The database can be seen as a mash up of information from different sources built to provide the core information required for selection and scientific engagement.

The NA-ARC website

Without a priori knowledge, exploration of the database is made possible by the NA-ARC website available at the URL:

<http://www.ifremer.fr/lpo/naarc>

A snapshot of the home page is shown in figure 1 (using the Safari browser). The website provides interactive visualization tools powered by modern web technologies. A menu on the left offers six main visualization panes: "Map", "Charts", "Time Series", "Data Explorer", "Tickets and Data Quality" and a "Profiles selection wizard". A non-exhaustive list of visualization tools is: map of profiles location, pie

Figure 1: The NA-ARC website homepage.

charts (distribution per DAC or data mode, ...), time series (of the distribution per year, the seasonal cycle sampling, ...), gauges (for tickets, availability of oxygen measurements, ...), bar charts of parameter measurements quality and two search engines to retrieve tickets information and visualize figures of temperature/salinity and possibly oxygen. All plots use bright colors and scalable vector graphics so that they respond to mouse events, support animation and more importantly can be printed with optimum resolution (other elements of the website layout have also been optimized for friendly printing). Figure 2 showcases some of these tools.

Each visualization tool is embedded into an independent module developed specifically for the website. These modules provide interaction methods with the data visualized. For instance one can modify the type of chart used to represent the data, toggle between number of profiles and floats, possibly save the chart as a figure file and add restrictions to the data set used by the module to generate custom chart on demand.

By default, all visualization tools use the entire database. The “Profiles selection wizard” makes possible user specific data mining. It helps users select and define restriction parameters on profile properties in order to create a virtual sub-set of profiles (fill a “cart”). Once the sub-set is defined, all visualization tools of the website are updated automatically using the “cart” selection and temperature/salinity sections and profiles figures can be scrolled in the “Data Explorer” pane. This provides a unique way to engage with Argo data and to start exploring a sub-set of profiles without downloading any single NetCDF file. If the user is satisfied with its collection of profiles, the “Profiles selection wizard” also offers the possibility to create a script file to download NetCDF profile files from GDAC ftp servers.

One more feature offered by the website is the persistent storage of the “cart”. The restriction parameters corresponding to the virtual “cart” (along with other layout parameters) are stored in the browser. This allows users to later revisit the website and eventually monitor changes to their sub-set of profiles.

The NA-ARC web API

All information provided by the website is served by the NA-ARC web API. The web API allows for users to access and mine the database from a script. This can be very powerful and provides a method for automatic processes. Here basic usage of the web API is presented. A detailed description of all available parameters and their usage, along with examples and output format descriptions can be found on the NA-ARC website online documentation.

A web API is an URL to which parameters can be added to obtain specific information from the system. The NA-ARC web API is accessible at: <http://www.ifremer.fr/lpo/naarc/api/v1/>

The API parameters can be sorted in three categories:

- parameters selecting a service (get, file, qwmo, doc, plan ...)
- parameters defining the service's functions and options (n,list,coord ...),

- parameters defining restrictions on profiles properties (year,dac,box,...)

For example, querying the API can take the following form:

<http://www.ifremer.fr/lpo/naarc/api/v1/?get=np>



Figure 2: Samples of the NA-ARC website visualization tools.

This query calls for the function “np” (number of profiles) provided by the service “get”. It returns the total number of profiles in the database (167,475 as of 2012/02/10). If one wants to obtain the number of profiles sorted by year, the option “by” can be used like: `[...]/?get=np&by=year`. This option can handle a secondary sorting key. For instance, the number of profiles per year and data mode would be retrieved using: `[...]/?get=np&by=year,dmode`. At this time, there are 9 functions available with the service ‘get’. They provide an extensive list of possibilities to describe and mine the database in a simple way.

The web API default output format is JSON (JavaScript Object Notation): an easily human readable format that can be handled by scripts (python, R). It does not require any a priori knowledge to be understood. Note that the web API can also output data as Matlab evaluable strings or CSV text files.

All services and functions use the entire database of profiles by default. They can be completed by restriction parameters to select a sub-set of profiles. This is where users can fully customize their requests and express their requirements. They are more than 20 restriction parameters available at this time. They allow restrictions on *meta* information, space, time and data quality (DAC name, WMO, profile parameters, years, date range, box, tickets, parameters QC and more). As a restriction parameter example, let us consider “around” which allows selecting profiles near a specific one. This can be useful in quality control procedures for instance. To select profiles in a circular radius of 300km sampled ± 30 days around the fifth cycle of float WMO 6900678 is as simple as adding “around=6900678,5,300,30” to a function call. Last, note that as many as required restriction parameters can be used to create a very specific sub-set of profiles. In the previous example, one would also select profiles with a correct quality flag on temperature using: “around=6900678,5,300,30&temp_qc=A,B”.

Conclusion

We hope the NA-ARC website and API will provide complementary services to help users engage with Argo data in the North Atlantic. From a scientist perspective, we have tried to extend the classic engagement workflow of selection/download of profile files with a more comprehensive set of data mining and visualization tools. The entire system is flexible so that more information and services could be implemented in the future, following users suggestions.

NOTEBOOK

Editorial Board

Laurence Crosnier

Sylvie Pouliquen

DTP Operator

Fabrice Messal

Articles

NAOS: preparing the new decade for Argo.

By P.-Y. Le Traon, F. D'Ortenzio, M. Babin, H. Claustre, S. Pouliquen, S. Le Reste, V. Thierry, P. Brault, M. Guigue, M. Le Menn

Ice, Atmosphere, Ocean Observing System: the EQUIPEX-funded IAOS project.

By the IAOS Team: C. Provost and J. Pelon, coordinators; P. Lattes scientific and technical project manager, J.C. Gascard, M. Calzas, F. Blouzon, A. Desautez, J. Descloitres, N. Sennéchaël, work package (co)-leaders, J.P. Pommereau, T. Foujols, A. Sarkissian, G. Ancellet, C. Drezen, A. Guillot, C. Guillerm, C. Berthold, N. Geyskens, A. Abchiche, N. Amarouche, L. Rey-Grange, J.-M. Nicolas

Autonomously profiling the nitrate concentrations in the ocean: the pronuts project.

By F. D'Ortenzio, S. Le Reste, H. Lavigne, F. Besson, H. Claustre, L. Coppola, A. Dufour, V. Dutreuil, A. Laës-Huon, E. Leymarie, D. Malardé, A. Mangin, C. Migon, P. Morin, A. Poteau, L. Prieur, P. Raimbault, P. Testor

EGO: Towards a global glider infrastructure for the benefit of marine research and operational oceanography.

By P. Testor, L. Mortier, J. Karstensen, E. Mauri, K. Heywood, D. Hayes, P. Alenius, A. Alvarez, C. Barrera, L. Beguery, K. Bernardet, L. Bertino, A. Beszczynska-Möller, T. Carval, F. Counillon, E. Dumont, G. Griffiths, P. M. Haugan, J. Kaiser, D. Kasis, G. Krahmann, O. Llinas, L. Merckelbach, B. Mourre, K. Nittis, R. Onken, F. D'Ortenzio, S. Pouliquen, A. Proelss, R. Riethmüller, S. Ruiz, T. Sherwin, D. Smeed, L. Stemmann, K. Tikka, J. Tintoré

Cirene: from cyclones to interannual timescales in the south-western tropical Indian Ocean.

By J. Vialard, Praveen Kumar B., N. C. Jourdain, and M. Bador

Use of ARGO floats to study the ocean dynamics south of Africa: what we have learned from the GoodHope project and what we plan within the SAMOC international programme.

By Sabrina Speich, Michel Arhan, Emanuela Rusciano, Vincent Faure, Michel Ollitrault, Annaïg Prigent, Sebastiaan Swart

Use of altimetric and wind data to detect the anomalous loss of SVP-type drifter's drogue

By M.-H. Rio

Surface salinity drifters for SMOS validation

By S. Morisset, G. Reverdin, J. Boutin, N. Martin, X. Yin, F. Gaillard, P. Blouch, J. Rolland, J. Font, J. Salvador

A new information and data mining tool for North Atlantic Argo data

By G. Maze

Contact :

Please send us your comments to the following e-mail address: webmaster@mercator-ocean.fr.

Next issue : October 2012